Molecular Pharmacology Fast Forward. Published on August 26, 2004 as doi:10.1124/mol.104.002337
This article has not been copyedited and formatted. The final version may differ from this version.

MOL 2337R

Signaling and ligand binding by recombinant neuromedin U receptors: evidence for dual coupling to $G\alpha_{q/11}$ and $G\alpha_{i}$ and an irreversible ligand-receptor interaction

Paul J. Brighton, Philip G. Szekeres, Alan Wise, and Gary B. Willars

Department of Cell Physiology and Pharmacology, University of Leicester, Leicester, UK (P.J.B. and G.B.W.) 7TMR Assay Development and Compound Profiling, GlaxoSmithKline, New Frontiers Science Park, Harlow, UK (P.G.S. and A.W.)

Molecular Pharmacology Fast Forward. Published on August 26, 2004 as DOI: 10.1124/mol.104.002337
This article has not been copyedited and formatted. The final version may differ from this version.

a) Running title:

Signaling by neuromedin U receptors

b) Correspondence

Address correspondence to: Dr. Gary. B. Willars, Department of Cell Physiology and Pharmacology, Medical Sciences Building, University of Leicester, University Road, LE1 9HN United Kingdom. Tel: +44 116 2523094. Fax: +44 116 2525045. E-mail: gbw2@le.ac.uk.

c)

Number of text pages:	34
Number of tables	1
Number of figures	11
Number of references	40
Number of words in the abstract	247
Number of words in the Introduction	736
Number of words in the Discussion	1515

d) Non-standard abbreviations:

[^{3}H]-InsP_x	total inositol phosphates
NmU	neuromedin U
NmU-R1	neuromedin U receptor 1
NmU-R2	neuromedin U receptor 2
hNmU-R1	human neuromedin U receptor 1
hNmU-R2	human neuromedin U receptor 2
MAPK	mitogen activating protein kinase
ERK	extracellular regulated kinase
hNmU-25	human neuromedin U-25
GPCR	G-protein coupled receptor
Ins(1,4,5)P_3	inositol (1,4,5) trisphosphate
KHB	Krebs'-based HEPES buffer
eGFP-$PH_{PLC\delta1}$	enhanced green fluorescent protein coupled to the plekstrin homology domain of phospholipase $C_{\delta1}$

F.I.U	fluorescent intensity units
HRP	horseradish peroxidase
NmU-8-Cy3B	neuromedin U-8 conjugated with Cy3B
$[Ca^{2+}]_i$	intracellular Ca^{2+} concentration

Molecular Pharmacology Fast Forward. Published on August 26, 2004 as DOI: 10.1124/mol.104.002337
This article has not been copyedited and formatted. The final version may differ from this version.

Abstract

The neuropeptide, neuromedin U (NmU), shows considerable structural conservation across species. Within the body it is widely distributed and in mammals has been implicated in physiological roles including the regulation of feeding, anxiety, pain, blood flow and smooth-muscle contraction. Recently, human NmU-25 (hNmU-25) and other NmU analogs were identified as ligands for two human orphan G-protein coupled receptors, subsequently named hNmU-R1 and hNmU-R2. These receptors have approximately 50% amino acid homology and, at least in mammalian species, NmU-R1 and NmU-R2 are expressed predominantly in the periphery and CNS respectively. Here, we have characterized signaling mediated by hNmU-R1 and hNmU-R2 expressed as recombinant proteins in HEK293 cells, particularly to define their G-protein coupling and the activation and regulation of signal transduction pathways. We show that these receptors couple to both $G\alpha_{q/11}$ and $G\alpha_{i}$. Activation of either receptor type causes a pertussis toxin-insensitive activation of both phospholipase C and mitogen activated-protein kinase and a pertussis toxin-sensitive inhibition of adenylyl cyclase with sub-nanomolar potency for each. Activation of phospholipase C is sustained but despite this capacity for prolonged receptor activation, repetitive application of hNmU-25 does not cause repetitive intracellular Ca^{2+} signaling by either recombinant receptors or those expressed endogenously in isolated smooth muscle cells from rat fundus. Using several strategies we show this to be a consequence of essentially irreversible binding of hNmU-25 to its receptors and that this is followed by ligand internalization. Despite structural differences between receptors there were no apparent differences in their activation, coupling or regulation.

Introduction

The neuropeptide, neuromedin U (NmU), was originally isolated from porcine spinal cord along with other neuromedins in the 1980s based on their ability to contract smooth-muscle. Purification and characterization of NmU identified two peptides with similar biological activity (Minamino et al., 1985), both of which contracted strips of rat uterus (hence the suffix 'U'). These peptides were an icosapentapeptide (NmU-25) and an octapeptide (NmU-8) identical to the C-terminus of NmU-25. The search for NmU in other species identified icosapentapeptides in human (hNmU-25), rabbit, dog, frog and chicken, a 23 amino acid version in rat and nonapeptides in guinea-pig and chicken. An octapeptide has also been identified in dog, which, as with porcine NmU-8, is most likely generated through cleavage at a di-basic Arg-Arg motif present in canine and porcine NmU-25 (for review see Brighton et al., 2004). Shorter versions of NmU are biologically active and indeed activity resides predominantly in the highly conserved C-terminus. In the rat, NmU-like immunoreactivity is widely distributed with highest levels in the anterior pituitary and gastrointestinal tract (Domin et al., 1987). Significant levels are also found in the brain, spinal cord and both the male and female genito-urinary tract (Domin et al., 1986). Circulating NmU has not been detected, suggesting that it acts as a neuropeptide or neuromodulator rather than a circulating hormone (Augood et al., 1988).

Despite an appreciation of the tissue distribution of NmU in several species and a detailed understanding of structure-activity relationships, its physiological roles remain to be defined precisely. NmU contracts smooth muscle in a tissue- and species-specific manner (Minamino et al., 1985; Bockman et al., 1989; Maggi et al., 1990; Westfall et al., 2001), regulates regional blood flow and blood pressure (Gardiner et al., 1990) and influences the pituitary-adrenal-cortical axis (Malendowicz et al., 1993). Intracerebroventricular administration of NmU mediates stress-responses and increases both arterial pressure and heart rate in conscious rats (Westfall et al., 2001; Chu et al., 2002) indicating a role in the regulation of sympathetic nervous activity and cardiovascular function. In rats, intracerebroventricular injection of NmU also decreases food intake and body weight (Howard et al, 2000; Kojima et al., 2000; Nakazato et al., 2000; Ivanov et al, 2002; Wren et al., 2002), and increases gross-locomotor activity, body temperature, heat

production and oxygen consumption (Howard et al., 2000; Nakazato et al., 2000). Interestingly leptin evokes the release of NmU from hypothalamic explants (Wren et al., 2002) suggesting that the effects of leptin on feeding, body weight and metabolism may also be mediated, at least in part, through NmU.

The recent identification of a human orphan G-protein-coupled receptor (GPCR) as a specific target for NmU (human neuromedin U-receptor 1; hNmU-R1) (Fujii et al., 2000; Hedrick et al., 2000; Hosoya et al., 2000; Howard et al., 2000; Kojima et al., 2000; Raddatz et al., 2000; Shan et al., 2000; Szekeres et al., 2000) and the subsequent identification of an additional receptor (human neuromedin U-receptor 2; hNmU-R2) (Hosoya et al., 2000; Howard et al., 2000; Raddatz et al., 2000; Shan et al., 2000) has greatly enhanced interest and understanding of NmU. Both receptors show characteristics of family 1 GPCRs and have approximately 50% amino acid homology. Recombinant NmU receptors elevate intracellular $[Ca^{2+}]$ ($[Ca^{2+}]_i$) with nM potency (Fujii et al., 2000; Hedrick et al., 2000; Hosoya et al., 2000; Howard et al., 2000; Kojima et al., 2000; Raddatz et al., 2000; Shan et al., 2000; Szekeres et al., 2000; Funes et al., 2002) although it is unclear whether they couple to other signaling pathways (Hosoya et al., 2000; Szekeres et al., 2000). The distribution of mRNA suggests that NmU-R1 and NmU-R2 are located predominantly but not exclusively in peripheral tissues and the CNS respectively (Hedrick et al., 2000; Hosoya et al., 2000; Howard et al., 2000; Raddatz et al., 2000; Shan et al., 2000; Szekeres et al 2000; Westfall et al., 2001). These distribution patterns have started to allow the assignment of particular physiological roles to the receptor sub-types. However, overlapping expression and the absence of selective ligands has made it difficult to define which receptors mediate specific responses and which intracellular signaling pathways are involved. The discovery of receptors for NmU presents the possibility of characterizing the cellular signaling pathways regulated by NmU. In the current study we have explored the signaling mediated by recombinantly expressed NmU receptors, examining their coupling to intracellular signal transduction pathways, desensitization profiles and potential differences between the receptor sub-types.

Molecular Pharmacology Fast Forward. Published on August 26, 2004 as DOI: 10.1124/mol.104.002337
This article has not been copyedited and formatted. The final version may differ from this version.

Materials and Methods

Materials. HEK293 cell culture reagents were from Gibco Life Technologies (Paisley, U.K.) and primary cell culture reagents were supplied by Cascade Biologics (Nottingham, U.K.). Cell culture plastic-ware was from NUNC (Roskilde, Denmark). Fluo-3-acetoxymethyl ester (fluo-3-AM) was supplied by TEF labs (Austin, TX, U.S.A.) and fluo-4-AM and pluronic F-127 by Molecular Probes Ltd (Leiden, The Netherlands). *myo*-[^{3}H]-Inositol (71Ci mmol^{-1}) and [^{125}I]-hNmU-25 (2000Ci mmol^{-1}) were from Amersham Biosciences (Little Chalfont, Bucks., U.K.), [^{3}H]-inositol 1,4,5-trisphosphate ([^{3}H]-Ins(1,4,5)P_3) (22Ci mmol^{-1}) and [^{3}H]-cAMP (34Ci mmol^{-1}) from NEN (Boston, MA, U.S.A.) and [^{35}S]-GTPγS (1250Ci mmol^{-1}) from PerkinElmer Life Sciences Inc. (Boston, MA, U.S.A.). Biocoat 384-well black-walled clear-bottomed microtitre plates were from Becton Dickinson (Bedford, MA, U.S.A.). Costar polypropylene 96-well plates, Unifilter 96-well white microplates with bonded Whatman GF/B filters and Microscint 20 scintillation fluid were all supplied by Packard (Boston, MA, U.S.A.). Emulsifier-safe scintillation fluid was supplied by Packard Bioscience (Groningen, The Netherlands). Protein A Sepharose beads were supplied by Amersham Biosciences (Uppsala, Sweden) and nitrocellulose membrane (Protran) was supplied by Schleicher and Schuell (Keene, NH, U.S.A.). The monoclonal antibody specific for $G\alpha_{q/11}$ (Bundey and Nahorski, 2001) was generated by Genosys Biotechnologies (Pampisford, U.K.) by inoculation of rabbits with the common C-terminal (positions 344-353) sequence (C)QLNLKEYNLV. Antibodies against $G\alpha_{i(1-3)}$ (SC-410) and $G\alpha_{s}$ (SC-823), ERK (SC-93) and phospho-ERK (SC-7383) were from Santa Cruz Biotechnology (Santa Cruz, CA, U.S.A.). The ECL Western blotting system was from Amersham Biosciences (Little Chalfont, Bucks., U.K.). The transfection reagents Genejuice and LipofectAMINE Plus were from Novagen (Madison, WI, U.S.A.) and Life Technologies (Paisley, U.K.) respectively. Protease inhibitor cocktail set 1 was from Calbiochem (Nottingham, U.K.). hNmU-25 was made at GlaxoSmithKline (Harlow, U.K.).

Other reagents were supplied by either Sigma Aldrich (Poole, U.K.), Fisher Scientific (Loughborough, U.K.), Merck (Darmstadt, Germany) or BDH Laboratory Supplies (Poole, U.K.).

Molecular Pharmacology Fast Forward. Published on August 26, 2004 as DOI: 10.1124/mol.104.002337
This article has not been copyedited and formatted. The final version may differ from this version.

Cell culture and creation of stable cell lines expressing hNmU-R1 or hNmU-R2. HEK293 cells were maintained in Minimum Essential Medium (MEM) with Earl's Salts supplemented with 10% fetal calf serum, non-essential amino acids and 50μg ml^{-1} gentamycin. Cells were maintained in 175cm^2 flasks at 37^oC in a 95%/5% air/CO_2 humidified environment. Cells for experimental use in multiwells or on coverslips were cultured on poly-D-lysine-coated surfaces. The DNA encoding hNmU-R1 was cloned into EcoR1/EcoRV and hNmU-R2 into Asp718/Bam HI of pCDN (Aiyar et al., 1994). Constructs were transfected using LipofectAMINE Plus and grown under selection (400μg ml^{-1} Geneticin). Clonal cell lines were expanded from single foci and screened by determination of hNmU-25-mediated elevation of $[Ca^{2+}]_i$ in fluo-3-AM-loaded cells using a fluorescence imaging plate reader (FLIPR), accumulation of total inositol phosphates ($[^3H]$-$InsP_x$), and Ins(1,4,5)P_3 production using both single-cell and population assays (see below). Relative expression levels were examined by the binding of $[^{125}I]$-hNmU-25 to membrane preparations using a concentration of ligand approximating to the K_d (see below). Single clones expressing either hNmU-R1 or hNmU-R2 were selected based on both similar expression levels and approximately equivalent functional responses mediated by hNmU-25 (10nM).

Dissociation and culture of rat stomach fundus smooth-muscle cells: cells were isolated by enzyme digestion and mechanical sheering of diced fundus from adult male Wistar rats (<300g) using a protocol originally optimised for the dissociation of pig coronary artery smooth muscle cells (Quayle et al., 1996). Animals were handled in accordance with the U.K. Animals (Scientific Procedures) Act, 1986. Following collection of cells by centrifugation (500g, 3min) they were re-suspended and cultured (37^oC; 5% CO_2) on untreated 25mm glass coverslips in Medium 231 supplemented with 5% smooth-muscle growth supplement, 50μg ml^{-1} streptomycin, 50 iu ml^{-1} penicillin and 50μg ml^{-1} gentamycin.

Binding of [^{125}I]-hNmU-25. *Membrane preparation:* confluent cell monolayers were harvested with phosphate buffered saline, collected by centrifugation (200g, 2min, 4^oC) and re-suspended in homogenization buffer (composition (mM) EDTA; 1, Tris-HCl; 10, PMSF 1, and benzamidine 200μg ml^{-1}, pH 7.4). After 15min on ice, cells

Molecular Pharmacology Fast Forward. Published on August 26, 2004 as DOI: 10.1124/mol.104.002337
This article has not been copyedited and formatted. The final version may differ from this version.

were homogenised, centrifuged (20000g, 4°C, 10min) and the pellets re-suspended in homogenization buffer at 1mg protein ml^{-1}. *[^{125}I]-hNmU-25 saturation binding*: experiments were performed in buffer (composition (mM, unless otherwise stated) Tris HCl pH 7.4, 20; $MgCl_2$, 5; Na-EGTA, 2; and bacitracin, 0.1mg ml^{-1}) in 100µl volumes in a 96-well format using 10µg of membrane and [^{125}I]-hNmU-25 at 0.1–1000pM. Non-specific binding was determined using 1µM hNmU-25 with a 5min pre-incubation period. After 1hr at room temperature, 100µl ice-cold 0.9% NaCl was added and the suspension rapidly filtered through 0.3% polyethylenimine pre-soaked Unifilter 96-well microplates with bonded Whatman GF/B filters. Recovered radioactivity was determined by standard liquid scintillation counting.

Determination of G-protein activation. *Membrane preparation*: cells were harvested with phosphate buffered saline, collected by centrifugation (200g, 5min, 4°C) and the pellet homogenised in lysis buffer (composition (mM) HEPES, 10; EDTA, 10; pH 7.4). This suspension was centrifuged (30000g, 15min, 4°C) and the final pellet homogenised in freezing buffer (composition (mM) HEPES, 10; EDTA, 0.1; pH 7.4). Protein concentration was adjusted to 1mg ml^{-1}. *[^{35}S]-GTPγS binding and immunoprecipitation of Gα-subunits*: determination of G-protein activation was by [^{35}S]-GTPγS binding and immunoprecipitation of specific Gα-subunits (Akam et al., 2001) using membranes (25µg) incubated with either 1µM (for $G\alpha_{q/11}$) or 10µM (for $G\alpha_i$ and $G\alpha_s$) GDP and 1nM [^{35}S]-GTPγS**.** Where appropriate, tubes contained 10µM GTPγS to determine non-specific binding and/or 10nM hNmU-25. Following incubation (2min, 37°C) the reaction was terminated with ice-cold buffer and membranes pelleted by centrifugation. Pellets were solubilised, pre-cleared and incubated overnight at 4°C with 5µl Gα-specific antisera (1:100 dilution). Immune complexes were isolated with Protein A Sepharose beads, collected by centrifugation and extensively washed. Beads were re-suspended in scintillation fluid and [^{35}S] determined.

Determination of phospholipase C activity

Total [^{3}H]-inositol phosphate ([^{3}H]-InsP$_x$) accumulation. Cell monolayers in 24-well plates were loaded with 3µCi ml^{-1} of *myo*-[^{3}H]-inositol for 48h and, if required, treated with 100ng ml^{-1} pertussis toxin for the last 20-24h. Cells were washed twice

with 1ml of Krebs'-based HEPES buffer (KHB) (composition (mM, unless otherwise stated): HEPES 10; $NaHCO_3$ 4.2, D-glucose 11.7; $MgSO_4.7H_2O$ 1.18; KH_2PO_4 1.18; KCl 4.69; NaCl 118; $CaCl_2.2H_2O$ 1.29; 0.01% w/v BSA, pH 7.4) and equilibrated at 37°C for 15min with 250µl KHB containing 10mM LiCl. For experiments here and elsewhere, Ca^{2+}-free conditions were obtained by the exclusion of $CaCl_2.2H_2O$ from the KHB. Cells were challenged with agonist and the reaction terminated with an equal volume of ice-cold, 1M trichloroacetic acid. [^{3}H]-InsP_x were extracted and separated by anion exchange chromatography (Willars and Nahorski, 1995).

Ins(1,4,5)P_3 mass generation. Cell monolayers in 24-well plates were washed with 1ml KHB and incubated at 37°C for 10min with 200µl KHB. Cells were challenged with 50µl KHB containing hNmU-25 as required. Reactions were terminated by the addition of an equal volume of 1M trichloroacetic acid. Ins(1,4,5)P_3 was extracted and determined using a radioreceptor assay (Willars and Nahorski, 1995) and related to cell protein content.

Single cell imaging of phospholipase C activity. The vector containing the fusion construct between the enhanced green fluorescent protein (eGFP) and the pleckstrin homology (PH) domain of phospholipase $C_{\delta 1}$ (eGFP-$PH_{PLC\delta 1}$) was generously provided by Professor T. Meyer (Stanford University, CA, U.S.A) and used to monitor phospholipase C activity in single cells as described (Nash et al., 2001). Briefly, cells on 25mm coverslips were transfected with 1µg of eGFP-$PH_{PLC\delta 1}$ plasmid cDNA using Genejuice transfection reagent. Cells were cultured for 48hr and coverslips mounted onto the stage of an Ultra*VIEW* confocal microscope (PerkinElmer Life Sciences, Cambridge, U.K.) with a X40 oil emersion objective and excited at 488nm using a Kr/Ar laser. Emitted light was collected above 510nm and images captured at approximately 1 sec^{-1}. The chamber volume was maintained at approximately 0.5ml and perfused (5ml min^{-1}) with KHB heated to 37°C with a Peltier unit. When cells were initially exposed to hNmU-25, perfusion was stopped and additions made directly to the cell chamber. Cytosolic fluorescence provides an index of Ins(1,4,5)P_3 levels and is expressed as the change in fluorescence relative to that in the 30s preceding agonist application.

Determination of $[Ca^{2+}]_i$

Molecular Pharmacology Fast Forward. Published on August 26, 2004 as DOI: 10.1124/mol.104.002337
This article has not been copyedited and formatted. The final version may differ from this version.

Confocal $[Ca^{2+}]_i$ imaging. Changes in $[Ca^{2+}]_i$ in single cells were performed essentially as described previously (Werry et al., 2002). Briefly, cells on 25mm coverslips were loaded with 5μM fluo-3-AM with 0.044% (w/v) pluronic F-127 for 1h (HEK293 cells) or 30min (rat fundus smooth muscle cells) at room temperature and imaged as described above. Addition of hNmU-25 and thapsigargin was by bath application in the absence of perfusion. Other agonists and changes in buffer were via perfusion of the chamber (see above). Cytosolic fluorescence provides an index of the $[Ca^{2+}]_i$ and is expressed as the change in fluorescence relative to that in the 30s preceding agonist application.

FLIPR analysis. Cells were seeded into 384-well microtitre plates at 10,000 cells $well^{-1}$ and cultured for 24hr. Cell counts were achieved by counting particles of 9.5-30μm with a Beckman Coulter Z-series cell counter (Beckman Coulter, Bucks, U.K.). Following loading (1μM fluo-4-AM in KHB for 1h at 37°C), cells were washed 3 times and incubated for 10min before assay on a FLIPR at 37°C. The response following agonist addition was taken as the maximum fluorescence intensity units (F.I.U) less the minimum immediately prior to addition.

Inhibition of forskolin induced cAMP accumulation.

Cell monolayers in 24-well plates were washed with 1ml KHB and incubated at 37°C for 10min with 1ml KHB. Buffer was aspirated and replaced by 200μl of buffer containing agonist at the required concentration. Following a 10min incubation at 37°C, a further 50μl of buffer containing both agonist at the required concentration and forskolin (final concentration, 10μM) was added. Following a further 10min incubation at 37°C, buffer was removed and reactions terminated with ice-cold 0.5M trichloroacetic acid. The cAMP was extracted using a method identical to that for the extraction of $Ins(1,4,5)P_3$ (Willars and Nahorski, 1995). The cAMP content was determined using a radioreceptor assay with binding-protein purified from calf adrenal glands (Brown et al., 1971) and related to cellular protein levels.

Determination of ERK activation. *Receptor activation and cell solubilization*: cells on 24-well plates were washed and equilibrated in KHB at 37°C. Cells were stimulated with 10nM hNmU-25 at 37°C and reactions terminated by aspiration and addition of ice-cold solubilization buffer (composition mM, (unless otherwise stated)

Tris, 100; EDTA, 10; NaCl, 150; NP40, 1% (v:v); SDS, 0.1%; deoxycholic acid, 5mg ml^{-1}; benzamidine, 200μg ml^{-1}; PMSF, 1; and protease inhibitor cocktail; pH 7.4). Cell lysates were pre-cleared by centrifugation (12000g, 10min, 4°C) and supernatant was adjusted to 3mg protein ml^{-1}. *Western blotting:* proteins (30μg) were separated by 10% SDS-PAGE, transferred onto nitocellulose membranes, blocked and probed for ERK. Blots were then stripped and re-probed for phospho-ERK (pERK). In each case visualization was achieved using HRP-conjugated secondary antibodies, ECL detection and autoradiography. Densitometric analysis of the autoradiographs was achieved with a Syngene (Cambridge, U.K.) Bio Imaging System using Genesnap-GeneGnome software (Syngene, Cambridge, UK) using only the density of p38 ERK (ERK 1) against which the antibody was raised.

Generation of fluorescently tagged porcine NmU-8 and binding to cells expressing either hNmU-R1 or hNmU-R2. *Generation of NmU-8-Cy3B*: Cy3B was attached to the N-terminus of porcine NmU-8 using Cy3B-NHS ester (Amersham, U.K.), following standard conditions as recommended by the manufacturer. The product (NmU-8-Cy3B) was purified by C18 reverse-phase HPLC, and mass confirmed by MALDI. *Imaging of NmU-8-Cy3B:* cells were seeded onto 25mm diameter poly-D-lysine coated glass coverslips and cultured for 24-48hr. Cells were washed with KHB and the coverslips mounted onto the stage of an Ultra*VIEW* confocal microscope. Cells were excited at 568 nm using a Kr/Ar laser and emitted light collected with a broad band RGB emission filter. NmU-8-Cy3B was added via bath application at a concentration of 10nM and images were taken at a rate of approximately 1 sec^{-1}. Where appropriate, KHB was perfused over the cells at a rate of 5ml min^{-1}. Temperature was controlled at 37°C with a Peltier unit, or at 12°C with a Peltier unit and perfusion of ice-cold buffer.

Data analysis. Concentration-response curves and saturation radioligand binding data were fitted using GraphPad Prism (GraphPad Prism Software, San Diego, CA, U.S.A) using a standard four-parameter logistic equation. All data shown are expressed as the mean of 3 experiments (unless otherwise stated) ± s.e.m. For representative data, experiments were also performed to an *n* of three or more.

Molecular Pharmacology Fast Forward. Published on August 26, 2004 as DOI: 10.1124/mol.104.002337
This article has not been copyedited and formatted. The final version may differ from this version.

Results

Expression of recombinant hNmU-R1 and hNmU-R2

The binding of [^{125}I]-hNmU-25 to membranes from the clonal cell lines expressing either hNmU-R1 or hNmU-R2 was saturable with the non-specific component representing approximately 50% of the total at saturating concentrations of [^{125}I]-hNmU-25. There was no specific binding to wild-type (non-transfected) HEK293 cells (data not shown). Saturation binding curves indicated B_{max} values of 4.88±0.33 pmol mg^{-1} and 1.95±0.16 pmol mg^{-1} for hNmU-R1 and hNmU-R2 respectively. These experiments also indicated K_d values of –9.87±0.05 $\log_{10}$ M (135pM) and –9.95±0.10 $\log_{10}$ M (112pM) for hNmU-R1 and hNmU-R2 respectively. However, it must be noted that given the characteristics of NmU binding that indicate a lack of reversibility (see below), these K_d values may be of limited value in describing the binding characteristics.

G-protein-coupling of hNmU-R1 and hNmU-R2 in cell membranes

Binding of [^{35}S]-GTPγS to immunoprecipitated $G\alpha_{q/11}$ (Fig. 1a) or $G\alpha_{i(1-3)}$ (Fig. 1c) increased by approximately 3-fold over basal upon activation of either hNmU-R1 or hNmU-R2 with 10nM hNmU-25. The binding of [^{35}S]-GTPγS to $G\alpha_s$ did not increase following activation of either receptor type (Fig. 1b) although activation of endogenously expressed β_2-adrenoceptors with 100μM noradrenaline resulted in an approximately 1.5-2 fold increase above basal levels (data not shown). Non-specific binding using 10μM GTPγS was ~20-50% of basal (unstimulated) [^{35}S]-GTPγS binding (Fig. 1). In additional cell lines expressing either hNmU-R1 or hNmU-R2 at 26% and 31% respectively of the level in cells used throughout the rest of the study (data not shown), 10nM NmU also increased [^{35}S]-GTPγS binding to $G\alpha_{i(1-3)}$ by approximately 2.5-3 fold over basal (Fig. 1d).

hNmU-25-mediated phosphoinositide signaling

In cells expressing either hNmU-R1 or hNmU-R2, 10nM hNmU-25 caused marked accumulations of [^{3}H]-$InsP_x$ against a Li^+-block of inositol monophosphatase activity (Fig. 2a) that continued until the furthest time tested (60min). Accumulation was biphasic, with a rapid phase (300-350% over basal min^{-1}) that became (at ~20s) slower (50-60% over basal min^{-1}) but sustained (Fig. 2b) suggesting a rapid but partial

Molecular Pharmacology Fast Forward. Published on August 26, 2004 as DOI: 10.1124/mol.104.002337
This article has not been copyedited and formatted. The final version may differ from this version.

desensitization of phospholipase C activity. Challenge of wild-type HEK293 cells with 10nM hNmU-25 did not result in accumulation of [^{3}H]-InsP_x (data not shown). The accumulation of [^{3}H]-InsP_x was concentration-dependent, with similar pEC_{50} values of 9.14±0.07 and 8.97±0.18 for hNmU-R1 or hNmU-R2 respectively (Figs. 2c and 2d). Pertussis toxin had no effect on hNmU-25-mediated accumulation of [^{3}H]-InsP_x in either cell line (Figs. 2c and 2d) indicating a lack of involvement of $G\alpha_{i/o}$ in NmU-mediated phospholipase C responses. In cells expressing hNmU-R1, challenge with 10nM hNmU-25 in the absence of extracellular Ca^{2+} had no effect on the bi-phasic profile of the accumulation of [^{3}H]-InsP_x but by 60min had reduced the accumulation to 40±10% (n=3) of that seen in the presence of extracellular Ca^{2+}.

Activation of either receptor type with 10nM hNmU-25 resulted in a rapid and marked increase in Ins(1,4,5)P_3 mass that peaked at 10s and declined to a lower but sustained phase (Fig. 3a).

Transfection of cells expressing either hNmU-R1 or hNmU-R2 with eGFP-$PH_{PLC\delta1}$ resulted in the expression of the construct and localization predominantly to the plasma membrane (Fig. 3b and c, panel A) due to the high affinity of the PH domain for PtdIns(4,5)P_2. Activation of either hNmU-R1 or hNmU-R2 with 10nM hNmU-25 resulted in the translocation of eGFP-$PH_{PLC\delta1}$ to the cytosol followed by a partial re-localization to the plasma membrane (Fig. 3b and c, panels B and C). This was reflected in analysis of cytosolic fluorescence intensity (Fig. 3b and c). Translocation to the cytosol is a consequence of the higher affinity of eGFP-$PH_{PLC\delta1}$ for Ins(1,4,5)P_3 than PtdIns(4,5)P_2 and therefore reflects cellular levels of Ins(1,4,5)P_3 (Nash et al., 2001).

hNmU-25-mediated Ca^{2+} signaling

Single-cell imaging of $[Ca^{2+}]_i$ in cells expressing either hNmU receptor revealed robust (2-3 fold over basal), rapid (5s) peaks followed by lower (1.2-1.4 fold over basal) sustained phases in response to 10nM hNmU-25 (Fig. 4a and b). Removal of extracellular Ca^{2+} had little effect on the peak elevation but abolished the sustained phase (data not shown). Removal of extracellular Ca^{2+} during the hNmU-25-mediated sustained elevation of $[Ca^{2+}]_i$ caused a reduction in $[Ca^{2+}]_i$ back to basal levels in hNmU-R1 and hNmU-R2 cell lines (data not shown). Pre-treatment of cells for 10min with the sarco/endoplasmic reticulum Ca^{2+}-ATPase inhibitor thapsigargin

(1μM) abolished the Ca^{2+} responses in both hNmU-R1 and hNmU-R2 expressing cells (data not shown).

Analysis of Ca^{2+} signaling by FLIPR demonstrated hNmU-25-mediated $[Ca^{2+}]_i$ profiles in populations consistent with those in single cells (Fig. 4c and d). The pEC_{50} values for the hNmU-25-mediated peak elevation of $[Ca^{2+}]_i$ in hNmU-R1 and hNmU-R2 cells were 9.41±0.09 and 9.37±0.06 respectively (Fig. 4e and f).

hNmU-25-mediated regulation of cAMP

Activation of either hNmU-R1 or hNmU-R2 with hNmU-25 resulted in the inhibition of forskolin (10μM) stimulated cAMP accumulation (Fig. 5) with pEC_{50} values of 10.10±0.16 and 10.06±0.17 in cells expressing hNmU-R1 or hNmU-R2 respectively. Pertussis-toxin treatment (20h, 100ng ml^{-1}) abolished this inhibition of forskolin-stimulated cAMP accumulation (Fig. 5). Addition of 10nM hNmU-25 did not increase cAMP in cells expressing either receptor in the presence or absence of the phosphodiesterase inhibitor, isobutylmethylxanthine (500μM) (data not shown). In contrast, challenge of endogenously expressed $G\alpha_s$-coupled β_2-adrenoceptors caused a 5-fold increase in cAMP above basal levels in the absence of isobutylmethylxanthine (data not shown).

Activation of ERK by hNmU-R1 and hNmU-R2

Challenge of either hNmU-R1 (Fig. 6a(i)) or hNmU-R2 (Fig. 6b(i)) with 10nM hNmU-25 did not alter cellular levels of ERK. However, hNmU-25 increased the level of pERK, which peaked after 5-10min of stimulation and then slowly declined (Fig. 6a(ii), 6b(ii); 6c). ERK phosphorylation following activation of either receptor subtype was unaffected by pertussis toxin (24h, 100ng ml^{-1}; data not shown).

Desensitization of hNmU-R and irreversible binding of hNmU-25 under physiological conditions

Single-cell $[Ca^{2+}]_i$ imaging demonstrated that following the stimulation of either hNmU-R1 or hNmU-R2 expressing cells with 10nM hNmU-25, perfusion with agonist-free buffer did not return the $[Ca^{2+}]_i$ to basal levels. Furthermore, re-application of 10nM hNmU-25 following this perfusion had no effect on $[Ca^{2+}]_i$ (Fig. 7a and b). Application of 100μM carbachol to activate endogenous $G\alpha_{q/11}$-coupled

muscarinic M_3 receptors also evoked a peak and plateau of $[Ca^{2+}]_i$ elevation that was similar to that evoked by 10nM hNmU-25 (Fig. 7c). Subsequent perfusion of agonist-free buffer reduced $[Ca^{2+}]_i$ to basal levels and re-application of 100μM carbachol resulted in a Ca^{2+} response that was 40±10% (n=34 cells) of the original (Fig. 7c). In hNmU-R1 expressing cells, the addition of 10nM hNmU-25 at 150s following 100μM carbachol resulted in a Ca^{2+} response of approximately 50±10% (n=26 cells) of that achieved by the addition of hNmU-25 to naïve cells (n=26 cells). However, if cells were washed (120s) with agonist-free buffer following 100μM carbachol, then 10nM hNmU-25 evoked a Ca^{2+} response that was 105±15% (n=45 cells) of that induced by addition of 10nM hNmU-25 to naïve cells. In contrast, application of 100μM carbachol at 150s following hNmU-25 evoked a Ca^{2+} response of that was only approximately 25% that of the initial hNmU-25 response irrespective of whether there had been a wash period (120s) or not following hNmU-25 application (n=37 and 47 cells respectively) (data not shown).

In primary isolates of rat fundus, individual smooth muscle cells that had been allowed to adhere to coverslips for several hours often showed robust contractions to stimulation with either 300μM UTP or 10nM hNmU-25 (data not shown). These contractions most often resulted in cell rounding and detachment from the coverslip. Cells that had been cultured for 5-7 days were more firmly adhered to the coverslip and robust contractions were rarely seen. However, in cells loaded with fluo-3 and imaged by confocal microscopy, either 300μM UTP (Fig. 8a) or 10nM hNmU-25 (Fig. 8b) evoked marked peak and plateau elevations of $[Ca^{2+}]_i$. Following stimulation, perfusion with agonist-free buffer reduced $[Ca^{2+}]_i$ to basal levels following stimulation with UTP (Fig. 8c) but not hNmU-25 (Fig. 8d). Furthermore, following this wash period (120s), re-application of UTP (Fig. 8c) but not hNmU-25 (Fig. 8d) resulted in a further elevation of $[Ca^{2+}]_i$.

Following hNmU-25, the inability of a wash with buffer to fully restore subsequent Ca^{2+} responses to either hNmU-25 or carbachol is suggestive of homologous and partial heterologous desensitization that either persists despite agonist removal or alternatively is a consequence of continued signalling by NmU receptors. The latter is consistent with the sustained accumulation of $[^3H]$-$InsP_x$ under a Li^+-block in HEK293 cells (see above), suggesting that heterologous desensitization could occur simply through, for example, depletion of a shared intracellular Ca^{2+}

Molecular Pharmacology Fast Forward. Published on August 26, 2004 as DOI: 10.1124/mol.104.002337
This article has not been copyedited and formatted. The final version may differ from this version.

store. Taken together, these data suggest that our wash protocol was not sufficient to remove receptor-bound hNmU-25. To further explore this we employed four complimentary approaches: the influence of washing on the accumulation of [^{3}H]-$InsP_x$; receptor crosstalk; the visualization of NmU binding using a fluorescently-labelled NmU and the ability of excess cold NmU to displace receptor-bound [^{125}I]-NmU.

The influence of washing cells to remove hNmU-25 on the accumulation of [^{3}H]-$InsP_x$. As an initial approach to explore the ability to remove receptor-bound hNmU-25, we examined the impact of extensively washing cells during the linear phase of accumulation of [^{3}H]-$InsP_x$ under a Li^+-block of inositol monophosphatase. Cells expressing hNmU-R1 were challenged with 10nM hNmU-25 and after 10min were either i) untreated or alternatively, the buffer removed and the cells washed (three times with 1ml buffer) before replacement of buffer ii) without or iii) with 10nM hNmU-25. Irrespective of the manipulation, the rate and extent of accumulation of [^{3}H]-$InsP_x$ was similar (Fig. 9a). Identical data were obtained using cells expressing hNmU-R2 (data not shown). This is in contrast to similar manipulations using 100μM carbachol, where removal of carbachol abolished further accumulation of [^{3}H]-$InsP_x$ (Fig. 9b).

Receptor crosstalk. As a second approach to examine whether receptor-bound hNmU-25 could be removed with buffer we made use of crosstalk between receptors coupled to $G\alpha_{q/11}$ and those coupled to either $G\alpha_s$ or $G\alpha_i$. As a consequence of such crosstalk, following activation of a $G\alpha_{q/11}$-coupled receptor, activation of either a $G\alpha_s$- or $G\alpha_i$-coupled receptor can, in some instances, result in the appearance or potentiation of Ca^{2+} signaling (Werry et al., 2003). Often the ongoing activation of $G\alpha_{q/11}$-coupled receptors is required for the crosstalk and this has the potential to reveal whether these receptors are active at the time of challenge of $G\alpha_s$- or $G\alpha_i$-coupled receptors. In HEK293 cells, challenge of an endogenous β_2-adrenoceptor with 10μM noradrenaline did not elevate $[Ca^{2+}]_i$ (Fig. 10a). However, following and in the continued presence of carbachol-mediated activation of the $G\alpha_{q/11}$-coupled muscarinic M_3 receptor, application of 10μM noradrenaline resulted in a robust elevation of $[Ca^{2+}]_i$ (Fig. 10a). Removal of carbachol by a 2min wash with KHB abolished the $[Ca^{2+}]_i$ response to a

Molecular Pharmacology Fast Forward. Published on August 26, 2004 as DOI: 10.1124/mol.104.002337
This article has not been copyedited and formatted. The final version may differ from this version.

subsequent application of noradrenaline (Fig. 10b) confirming the need for ongoing activation of the $G\alpha_{q/11}$-coupled receptor to mediate receptor crosstalk. Challenge of cells with 10μM noradrenaline following and in the continued presence of 10nM hNmU-25 also provoked a robust elevation of $[Ca^{2+}]_i$ in cells expressing hNmU-R1 (Fig. 10c). Washing the cells with KHB for 3min following challenge with 10nM hNmU-25 did not abolish the subsequent $[Ca^{2+}]_i$ response to noradrenaline (Fig. 10d) suggesting that hNmU-R1 was still active. Data obtained using cells expressing hNmU-R2 were identical to those obtained using cells expressing hNmU-R1 (data not shown).

Binding of fluorescently-labelled NmU. As a third approach to determine whether a wash with KHB is sufficient to remove receptor-bound hNmU-25, we used porcine NmU-8 with an *N*-terminally conjugated fluorophore, Cy3B (NmU-8-Cy3B; 10nM). In studies based on $[^3H]InsP_x$ accumulation, NmU-8-Cy3B was equipotent with both unlabelled hNmU-25 and porcine NmU-8 (Table 1).

Addition of NmU-8-Cy3B to cells expressing hNmU-R1 resulted in an immediate appearance of intense fluorescence localized to the plasma membrane (Fig. 11a(ii)). No fluorescence was observed following an identical addition to wild-type HEK293 cells (data not shown). At 1min following the addition of NmU-8-Cy3B, the addition of 1μM hNmU-25 did not result in a loss of plasma membrane fluorescence in hNmU-R1 expressing cells (Fig. 11b(i and ii)). Furthermore, following addition of 10nM NmU-8-Cy3B at 12°C (to block receptor internalization), continuous perfusion of cells with KHB (5ml min^{-1}) did not diminish plasma membrane fluorescence (Fig. 11c(i and ii)). Addition of 1μM hNmU-25 prior to the addition of NmU-8-Cy3B abolished the appearance of plasma membrane fluorescence in hNmU-R1 expressing cells (Fig. 11d(ii)).

Several alternative wash-protocols were used in an attempt to remove bound NmU-8-Cy3B (data not shown). These included increasing the salt concentration of the KHB (up to 200mM NaCl), the addition of acetic acid (up to 50mM), and reducing the buffer pH with HCl. Only when the buffer was reduced to pH 2.0 was there any loss of plasma membrane fluorescence. The loss of membrane fluorescence was immediate and full. Following a return of the cells to buffer at pH 7.4, membrane fluorescence re-appeared only following the re-addition of NmU-8-Cy3B. This wash

Molecular Pharmacology Fast Forward. Published on August 26, 2004 as DOI: 10.1124/mol.104.002337
This article has not been copyedited and formatted. The final version may differ from this version.

and re-binding procedure could be carried out at least three times without any discernable reduction in the fluorescence associated with the membrane in the presence of NmU-8-Cy3B at pH 7.4 (data not shown). However, even in the absence of any pre-stimulation this pH 2.0 wash resulted in a marked reduction in both $[Ca^{2+}]_i$ and [^{3}H]-$InsP_x$ responses to either hNmU-25 or carbachol (data not shown). At 37^{o}C (rather than 12^{o}C), addition of NmU-8-Cy3B also resulted in membrane fluorescence (Fig. 11e(i)) that could not be removed using KHB. Furthermore, after approximately 5min (300s), membrane fluorescence began to reduce coincident with the appearance of punctuate fluorescence within the cell (Fig. 11e(ii)) indicating internalization of the ligand. By approximately 8-10min, cellular fluorescence was almost exclusively punctate and cytosolic (Fig. 11e(iii)). All experiments with NmU-8-Cy3B were repeated in cells expressing hNmU-R2 and identical results were obtained (data not shown).

Displacement of pre-bound [^{125}I]-hNmU-25. As a final approach to examine the possible irreversible binding of NmU, we pre-bound [^{125}I]-hNmU-25 to membranes prepared from cells expressing either hNmU-R1 or hNmU-R2. Membranes (10μg) were incubated for 1h at room temperature with 150pM [^{125}I]-hNmU-25 to label approximately 50% of the receptors. An excess of unlabelled hNmU-25 (1μM) was then added and the amount of [^{125}I]-hNmU-25 remaining bound over the next hour was determined. The pre-binding of [^{125}I]-hNmU-25 resulted in the specific binding of approximately 2,600 d.p.m.. The addition of unlabelled hNmU-25 did not reduce the amount of bound [^{125}I]-hNmU-25 (100$\pm$5% remaining bound after 1h).

Molecular Pharmacology Fast Forward. Published on August 26, 2004 as DOI: 10.1124/mol.104.002337
This article has not been copyedited and formatted. The final version may differ from this version.

Discussion

The current study characterizes many aspects of the signaling profiles of the two human receptors for the neuropeptide, NmU. Using HEK293 cells with stable expression of either hNmU-R1 or hNmU-R2 we demonstrate coupling to both $G\alpha_{q/11}$ and $G\alpha_i$ G-proteins and that activation of these receptors results in robust phosphoinositide and Ca^{2+} signaling and in the inhibition of forskolin-stimulated accumulations of cAMP.

It is clear from the functional screening assays that hNmU-R1 and hNmU-R2 of human and rodent origin are able to mediate intracellular Ca^{2+} signaling with potency in the nM range (Fujii et al., 2000; Hedrick et al., 2000; Hosoya et al., 2000; Howard et al., 2000; Kojima et al., 2000; Raddatz et al., 2000; Shan et al., 2000; Szekeres et al., 2000; Funes et al., 2002). For hNmU-R1 this has been shown to be associated with phosphoinositide hydrolysis (Raddatz et al., 2000; Szekeres et al., 2000). Here we demonstrate that agonist activation of either hNmU-R1 or hNmU-R2 with hNmU-25 caused accumulations of $[^3H]$-$InsP_x$ for at least 1h against a Li^+-block of inositol monophosphatase activity. Furthermore, studies on cell populations demonstrated rapid, transient elevations of $[Ca^{2+}]_i$ that quickly subsided to small but sustained elevations. hNmU-25-mediated accumulations of $[^3H]$-$InsP_x$ and elevations of $[Ca^{2+}]_i$ were potent, each with EC_{50} values of approximately 1nM for both receptor sub-types. The sustained accumulation of $[^3H]$-$InsP_x$ over at least 1hr of agonist stimulation indicates that neither hNmU-R1 nor hNmU-R2 is subject to a rapid and full desensitization. However, closer examination over the first few minutes of stimulation revealed a bi-phasic accumulation consisting of an initial rapid but transient accumulation followed by a slower but sustained accumulation. This early switch from rapid to slower accumulation indicates a reduction in phospholipase C activity (Wojcikiewicz et al., 1993) consistent with a rapid but partial desensitization of signaling. This pattern is also consistent with a variety of other phospholipase C coupled receptors (Wojcikiewicz et al., 1993; Willars and Nahorski, 1995). Whilst the mechanism of desensitization is unclear an obvious candidate is receptor-G-protein uncoupling following agonist-dependent receptor phosphorylation by G-protein receptor kinases or second messenger-dependent kinases. Although the level of $Ins(1,4,5)P_3$ is determined by both its generation and metabolism, the peak and

plateau of hNmU-25-mediated increases in this second messenger is also consistent with a rapid but partial desensitization of signaling.

The similarity of the EC_{50} values for both $Ins(1,4,5)P_3$ accumulation and elevation of $[Ca^{2+}]_i$ are consistent with a tight coupling between these two events. Further, our single cell imaging of $[Ca^{2+}]_i$ in fluo-3-AM loaded cells and $Ins(1,4,5)P_3$ using the eGFP-$PH_{PLC\delta1}$ biosensor (Nash et al., 2001) demonstrate that these events are temporally similar and reflective of the average signals generated by the study of cell populations. The initial hNmU-25-mediated Ca^{2+} signaling arises from a thapsigargin-sensitive intracellular store whilst the sustained component is dependent on a transmembrane $[Ca^{2+}]$ gradient, most likely reflecting capacitative Ca^{2+} entry.

In our initial attempt to examine the potential desensitization of hNmU-25-mediated Ca^{2+} signaling using classical re-challenge protocols, a second addition of hNmU-25, following an initial challenge and wash, failed to elevate $[Ca^{2+}]_i$. This was also true of NmU-mediated Ca^{2+} signaling in cultured rat fundus smooth muscle cells suggesting that endogenously expressed receptors behave similarly. Although such behaviour could be a consequence of desensitization, this is totally inconsistent with the sustained plateau of $[Ca^{2+}]_i$ elevation in HEK293 cells and smooth muscle cells and the sustained accumulation of $[^3H]$-$InsP_x$ in HEK293 cells. These data suggest that our wash protocol was unable to remove high-affinity hNmU-25 binding to its receptors. This was confirmed for recombinant hNmU-R1 and hNmU-R2 using a variety of approaches, namely: the sustained accumulation of $[^3H]$-$InsP_x$ despite attempts to remove the ligand; the phenomenon of crosstalk between $G\alpha_{q/11}$ and $G\alpha_s$-coupled receptors; the irreversible binding of fluorescently labelled NmU (NmU-8-Cy3B) and; the inability of excess hNmU-25 to displace pre-bound $[^{125}I]$-hNmU-25. Although slightly acidic washes (pH 4-5) are often used to remove peptide ligands these, as with the endothelin-A receptor (Hilal-Dandan et al., 1996), proved ineffective in the removal of NmU-8-Cy3B from either hNmU-R1 or hNmU-R2. Indeed, only highly acidic washes ($\leq$pH 2) were able to remove NmU-8-Cy3B and although re-binding was possible, such acidity alone not surprisingly influenced cell signaling making it impossible to study further the desensitization using re-challenge protocols.

Interestingly, at 37^{o}C there was a substantial internalization of the fluorescently-labelled NmU over relatively short time-frames. Given the clear high-

affinity binding of NmU, this almost certainly reflects receptor internalization. However, substantial receptor internalization is somewhat in contrast to the sustained linear accumulation of [^{3}H]-InsP$_x$ between 1 and 60min even following removal of free hNmU-25 by washing. This suggests that the recycling of receptors and binding of additional hNmU-25 is unlikely to be required for sustained signaling and that sufficient active receptors either remain at the cell surface or are returned (with or without ligand). Further studies are required to distinguish these possibilities. Another possibility is that internalized receptors continue signaling and although it has been demonstrated that internalized muscarinic receptors cannot contribute to phosphoinositide turnover (Sorenson et al., 1997), whether this is true of all receptors in all circumstances is essentially unknown. As with many other peptide ligands such as endothelin A (Hilal-Dandan et al., 1996) and substance P (Schmidlin et al, 2001) the irreversible interaction of hNmU-25 with its receptors has implications on the function and regulation of its receptors. The physiological consequence of irreversible binding is unclear but may limit the responsiveness of the receptors to repeat agonist challenge.

GPCR-mediated activation of MAP kinase by both recombinant and endogenous receptors is well documented but mechanistically complex (Belcheva and Coscia, 2002). Here we show that hNmU-25-mediated activation of ERK is pertussis toxin-insensitive suggesting that G$\alpha_{q/11}$ coupling to phosphoinositide and Ca^{2+} signaling may be responsible. This is consistent with a variety of other receptors (Belcheva and Coscia, 2002). For some GPCRs (Daaka et al., 1998) but not all (Budd et al., 1999), internalization appears to be a requirement for activation of MAP kinase. Although our data indicate rapid internalization of both hNmU-R1 and hNmU-R2 within 4-5min of addition, the consequence of this internalization in the activation and regulation of signaling pathways, including the MAP kinase pathway remain to be established.

hNmU-25-mediated accumulation of [^{3}H]-InsP$_x$ by either hNmU-R1 or R2 is also insensitive to pertussis toxin demonstrating a lack of involvement of G$\alpha_{i/o}$ in this response. This is consistent with the pertussis toxin-insensitive Ca^{2+} signaling by both hNmU-R1 and hNmU-R2 (Raddatz et al., 2000; Shan et al., 2000; Szekeres et al., 2000) and indicates a G$\alpha_{q/11}$-mediated activation of phospholipase C. The direct coupling of both receptors to G$\alpha_{q/11}$ was confirmed by showing an hNmU-25

dependent increase in binding of [^{35}S]-GTPγS to this G-protein. These studies also demonstrated activation of $G\alpha_i$ by both receptors. Potential differences in the ability of antibodies to immunoprecipitate the different G-protein α-subunits means that we are unable to directly compare the levels of $G\alpha_{q/11}$ and $G\alpha_i$ activation. However, both receptor sub-types were able to inhibit forskolin-stimulated cAMP accumulation thereby demonstrating functional relevance of $G\alpha_i$ activation. The coupling of GPCRs to multiple G-proteins has, of course, been reported previously (for review see Hermans, 2003). Although the promiscuous coupling of GPCRs to G-proteins can be the consequence of aspects such as high-receptor expression levels or the agonist used, such promiscuity appears to be a physiological reality for a number of receptors (Hermans, 2003). In our studies we were also able to show the activation of $G\alpha_i$ using the immunoprecipitation protocol in membranes from additional hNmU-R clonal cell lines that expressed lower levels of receptor. Furthermore, both hNmU-R1 and hNmU-R2 inhibited forskolin-stimulated cAMP accumulation more potently than the elevation of Ca^{2+} or accumulation of [^{3}H]-InsP_x, again suggesting that this coupling may not be simply a consequence of high levels of receptor expression. Previously hNmU-25 has been reported to partially inhibit forskolin-stimulated cAMP accumulation in CHO cells with stable expression of hNmU-R2 (Hosoya et al., 2000), whilst activation of transiently expressed hNmU-R1 in HEK293 cells has no affect on either the basal or forskolin-stimulated levels of cAMP (Szekeres et al., 2000). Whether this dual coupling is true of any endogenously expressed hNmU receptors, and its physiological and therapeutic relevance, remains to be established.

In summary, we have shown that activation of human NmU receptors recombinantly expressed in HEK293 cells results in the activation of both phospholipase C and inhibition of adenylyl cyclase as demonstrated by increases in $[Ca^{2+}]_i$, Ins(1,4,5)P_3 and [^{3}H]-InsP_x accumulation and by a reduction in forskolin-elevated cAMP respectively. Furthermore, by directly assessing the coupling of G-proteins we have demonstrated that the activation of these pathways is the result of the dual coupling to both $G\alpha_{q/11}$ and $G\alpha_i$ G-proteins, whilst, consistent with a lack of increase in basal levels of cAMP upon receptor activation, no coupling is observed to $G\alpha_s$. We have also demonstrated that both hNmU-R1 and R2 activate MAP kinase. Finally, our data clearly demonstrate that NmU binding is of high affinity and that it binds essentially irreversibly under physiological conditions and that this binding is

followed rapidly by internalization. Despite structural differences between the two hNmU-receptor subtypes these studies have not revealed differences in the signaling properties of these two receptor types.

Acknowledgments

The authors would like to thank J. Scott and M. Ruediger (GlaxoSmithKline, Harlow, UK) for the generation and purification of Cy3B-NmU-8. We also thank both E. Appelbaum and E. Dul (GEPB, Upper Merion, Philadelphia, PA) for generating the stable cell lines and N. Elshourbagy and U. Shabon (Gene Cloning and expression Proteomics, GlaxoSmithKline, Harlow, UK) for cloning the receptors. We also express our thanks to S. Ratcliffe (GlaxoSmithKline, Harlow, UK) for supplying hNmU-25 and F. McKay (GlaxoSmithKline, Harlow, UK) for help in using the FLIPR. Financial support of the Biotechnology and Biological Sciences Research Council (grant 01/A4/C/07909), the Wellcome Trust (equipment grant 061050 for the purchase of the Ultra*VIEW* confocal microscope) and GlaxoSmithKline (Harlow, UK) is gratefully acknowledged.

Molecular Pharmacology Fast Forward. Published on August 26, 2004 as DOI: 10.1124/mol.104.002337
This article has not been copyedited and formatted. The final version may differ from this version.

References

Aiyar N, Baker E, Wu HL, Nambi P, Edwards RM, Trill JJ, Ellis C, and Bergma DL (1994) Human AT_1 receptor is a single-copy gene-characterization in a stable cell-line. *Mol Cell Biochem* **131:** 75-86.

Akam EC, Challiss RAJ and Nahorski SR (2001) $G_{q/11}$ and $G_{i/o}$ activation profiles in CHO cells expressing human muscarinic acetylcholine receptors: dependence on agonist as well as receptor-subtype. *Brit J Pharmacol* **132:** 950-958.

Augood SJ, Keast JR, and Emson PC (1988) Distribution and characterization of neuromedin-U-like immunoreactivity in rat-brain and intestine and in guinea-pig intestine. *Regul Peptides* **20:** 281-292.

Belcheva MM, and Coscia CJ (2002) Diversity of G-protein-coupled receptor signaling pathways to ERK/MAP kinase. *Neurosignals* **11:** 34-44.

Bockman CS, Abel PW, Hicks JW, and Conlon JM (1989) Evidence that neuromedin-U may regulate gut motility in reptiles but not in mammals. *Eur J Pharmacol* **171:** 255-257.

Brighton PJ, Szekeres PG, and Willars GB (2004) Neuromedin U and its receptors: structure, function and physiological roles. *Pharmacol Revs* **56:** 231-248.

Brown BL, Albano JDM, Ekins RP, Sgherzi AM, and Tampion W (1971) A simple and sensitive saturation assay method for the measurement of adenosine 3'5'-cyclic monophosphate. *Biochem J* **121:** 561-562.

Budd DC, Rae A, and Tobin AB (1999) Activation of the mitogen-activated protein kinase pathway by a $G_{q/11}$-coupled muscarinic receptor is independent of receptor internalization. *J Biol Chem* **274:** 12355-12360.

Bundey RA and Nahorski SR (2001) Homologous and heterologous uncoupling of muscarinic M_3 and α_{1B} adrenoceptors to G $\alpha_{q/11}$ in SH-SY5Y human neuroblastoma cells. *Brit J Pharmacol* **134:** 257-264.

Chu CP, Jin QH, Kunitake T, Kato K, Nabekura T, Nakazato M, Kanagawa K, and Kannan H (2002) Cardiovascular actions of central neuromedin U in conscious rats. *Regul Peptides* **105:** 29-34.

Daaka Y, Luttrell LM, Ahn S, Della Rocca GJ, Ferguson SSG, Caron MG, and Lefkowitz RJ (1998) Essential role for G-protein coupled receptor endocytosis in the activation of MAP kinase. *J Biol Chem* **273:** 685-688.

Domin J, Ghatei MA, Chohan P, and Bloom SR (1986) Characterization of neuromedin-U like immunoreactivity in rat, porcine guinea-pig and human-tissue extracts using a specific radioimmunoassay. *Biochem Biophys Res Commun* **140:** 1127-1134.

Domin J, Ghatei MA, Chohan P, and Bloom SR (1987) Neuromedin U – A study of its distribution in the rat. *Peptides* **8:** 779-784.

Fujii R, Hosoya M, Fukusumi S, Kawamata Y, Habata Y, Hinuma S, Onda H, Nishimura O, and Fujino M (2000) Identification of neuromedin U as the cognate ligand of the orphan G-protein-coupled receptor FM-3. *J Biol Chem* **275:** 21068-21074.

Funes S, Hedrick JA, Yang SJ, Shan LX, Bayne M, Monsma FJ, and Gustafson EL (2002) Cloning and characterization of murine neuromedin U receptors. *Peptides* **23:** 1607-1615.

Gardiner SM, Compton AM, Bennett T, Domin J, and Bloom SR (1990) Regional hemodynamic-effects of neuromedin-U in conscious rats. *Am J Physiol* **258:** R32-R38.

Hedrick JA, Morse K, Shan LX, Qiao XD, Pang L, Wang S, Laz T, Gustafson EL, Bayne M, and Monsma FJ (2000) Identification of a human gastrointestinal tract and immune system receptor for the peptide neuromedin U. *Mol Pharmacol* **58:** 870-875.

Hermans E (2003) Biochemical and pharmacological control of the multiplicity of coupling at G-protein-coupled receptors. *Pharmacol Therap* **99:** 25-44.

Hilal-Dandan R, Villegas S, Gonzalez A, and Brunton LL, (1997) The quasi-irreversible nature of endothelin binding and G-protein-linked signaling in cardiac myocytes. *J Pharmacol Exp Ther* **281:** 267-273.

Hosoya M, Moriya T, Kawamata Y, Ohkubo S, Fujii R, Matsui H, Shintani Y, Fukusumi S, Habata Y, Hinuma S, Onda H, Nishimura O, and Fujino M (2000) Identification and functional characterization of a novel subtype of neuromedin U receptor. *J Biol Chem* **275:** 29528-29532.

Howard AD, Wang RP, Pong SS, Mellin TN, Strack A, Guan XM, Zeng ZZ, Williams DL, Feighner SD, Nunes CN, Murphy B, Stair JN, Yu H, Jiang QP, Clements MK, Tan CP, McKee KK, Hreniuk DL, McDonald TP, Lynch KR, Evans JF, Austin CP, Caskey CT, Van Der Ploeg LHT, and Liu QY (2000) Identification of

receptors for neuromedin U and its role in feeding. *Nature* **406:** 70-74.

Ivanov TR, Lawrence CB, Stanley PJ, and Luckman SM (2002) Evaluation of neuromedin U actions in energy homeostasis and pituitary function. *Endocrinology* **143:** 3813-3821.

Kojima M, Haruno R, Nakazato M, Date Y, Murakami N, Hanada R, Matsuo H, and Kangawa K (2000) Purification and identification of neuromedin U as an endogenous ligand for an orphan receptor GPR66 (FM3). *Biochem Biophys Res Commun* **276:** 435-438.

Maggi CA, Patacchini R, Giuliani S, Turini D, Barbanti G, Rovero P, and Meli A (1990) Motor response of the human isolated small-intestine and urinary-bladder to porcine neuromedin U-8. *Brit J Pharmacol* **99:** 186-188.

Malendowicz KA, Nussdorfer GG, Nowak KW, and Mazzocchi G (1993) Effects of neuromedin U-8 on the rat pituitary-adrenocortical axis. *In Vivo* **7**: 419-422.

Minamino N, Kangawa K, and Matsuo H (1985) Neuromedin U-8 and U-25: novel uterus stimulating and hypertensive peptides identified in porcine spinal cord. *Biochem Biophys Res Commun* **130:** 1078-1085.

Nakazato M, Hanada R, Murakami N, Date Y, Mondal MS, Kojima M, Yoshimatsu H, Kangawa K, and Matsukura S (2000) Central effects of neuromedin U in the regulation of energy homeostasis. *Biochem Biophys Res Commun* **277:** 191-194.

Nash MS, Young KW, Willars GB, Challiss RAJ, and Nahorski SR (2001) Single cell imaging of graded Ins(1,4,5)P_3 production following G-protein-coupled receptor activation. *Biochem J* **356:** 137-142.

Quayle JM, Dart C, and Standen NB (1996) The properties and distribution of inward rectifier potassium currents in pig coronary arterial smooth muscle. *J Physiol* **494:** 715-726.

Raddatz R, Wilson AE, Artymyshyn R, Bonini JA, Borowsky B, Boteju LW, Zhou SQ, Kouranova EV, Nagorny R, Guevarra MS, Dai M, Lerman GS, Vaysse PJ, Branchek TA, Gerald C, Forray C, and Adham N (2000) Identification and characterization of two neuromedin U receptors differentially expressed in peripheral tissues and the central nervous system. *J Biol Chem* **275:** 32452-32459.

Schmidlin F, Dery O, DeFea KO, Slice L, Patierno S, Sternini C, Grady EF, and Bunnett NW (2001) Dynamin and rab5a-dependent trafficking and signalling of the neurokinin 1 receptor. *J Biol Chem* **276:** 25427-25437.

Shan LX, Qiao XD, Crona JH, Behan J, Wang S, Laz T, Bayne M, Gustafson EL, Monsma FJ, and Hedrick, JA (2000) Identification of a novel neuromedin U receptor subtype expressed in the central nervous system. *J Biol Chem* **275:** 39482-39486.

Sorenson SD, McEwan EL, Linseman DA, and Fisher SK (1997) Agonist-induced endocytosis of muscarinic cholinergic receptors: relationship to stimulated phosphoinositide turnover. *J Neurochem* **86:** 1473-1483.

Szekeres PG, Muir AI, Spinage LD, Miller JE, Butler SI, Smith A, Rennie GI, Murdock PR, Fitzgerald LR, Wu HL, McMillan LJ, Guerrera S, Vawter L, Elshourbagy NA, Mooney JL, Bergsma DJ, Wilson S, and Chambers JK (2000) Neuromedin U is a potent agonist at the orphan G-protein-coupled receptor FM3. *J Biol Chem* **275**: 20247-20250.

Westfall TD, McCafferty GP, Pullen M, Gruver S, Sulpizio AC, Aiyar VN, Disa J, Contino LC, Mannan IJ, and Hieble JP (2001) Characterisation of neuromedin U effects in canine smooth-muscle. *J Pharmacol Exp Ther* **301:** 987-992.

Werry TD, Christie MI, Dainty IA, Wilkinson GF, and Willars GB (2002) Ca^{2+} signalling by recombinant human CXCR2 chemokine receptors is potentiated by P2Y nucleotide receptors in HEK cells. *Brit J Pharmacol* **135:** 1199-1208.

Werry TD, Wilkinson GF, and Willars GB (2003) Mechanisms of cross-talk between G-protein-coupled receptors resulting in enhanced release of intracellular Ca^{2+} *Biochem J* **374:** 281-296.

Willars GB and Nahorski SR (1995) Quantitative comparisons of muscarinic and bradykinin receptor-mediated Ins(1,4,5)P_3 accumulation and Ca^{2+} signalling in human neuroblastoma cells *Brit J Pharmacol* **114:** 1133-1142.

Wojcikiewicz RJH, Tobin AB, and Nahorski SR (1993) Desensitization of cell signalling mediated by phosphoinositidase-C. *Trends Pharmacol Sci* **14:** 279-285.

Wren AM, Small CJ, Abbott CR, Jethwa PH, Kennedy AR, Murphy KG, Stanley SA, Zollner AN, Ghatei MA, and Bloom SR (2002) Hypothalamic actions of neuromedin U. *Endocrinology* **143:** 4227-4234.

Molecular Pharmacology Fast Forward. Published on August 26, 2004 as DOI: 10.1124/mol.104.002337
This article has not been copyedited and formatted. The final version may differ from this version.

Figure Legends

Figure 1. G-protein coupling of hNmU-R1 and hNmU-R2. Membrane preparations (25μg) from cells expressing either hNmU-R1 or hNmU-R2 were incubated in the presence of GDP (1μM for $G\alpha_{q/11}$ and 10μM for $G\alpha_{i(1-3)}$ and $G\alpha_s$), 1nM [^{35}S]-GTPγS and where applicable hNmU-25 (10nM) (Stimulated). Non-specific binding (NSB) was determined using 10μM GTPγS. Immunoprecipitation was carried out using antibodies against specific Gα subunits as indicated and associated [^{35}S] determined. The binding of [^{35}S]-GTPγS to $G\alpha_{i(1-3)}$ subunits using membranes prepared from additional lower expressing clones is also shown (d). All data are mean±s.e.m., n=4.

Figure 2. hNmU-R1- and hNmU-R2-mediated accumulation of [^{3}H]-InsP$_x$. Cells expressing either hNmU-R1 (□) or hNmU-R2 (o) were seeded into 24-well plates and loaded with [^{3}H]-*myo*-inositol for 48h. a) Cells were challenged with 10nM hNmU-25 for varying lengths of time ranging from 0-3600s (60min) in the presence of a 10mM Li^+-block of inositol monophosphatase activity. b) Detail from a) showing the accumulation of [^{3}H]-InsP$_x$ over the first 180s of agonist stimulation. Concentration-response curves for the accumulation of [^{3}H]-InsP$_x$ following activation of either hNmU-R1 (c) or hNmU-R2 (d) by hNmU-25. Cells were challenged under Li^+-block for 60min. The pEC_{50} values were 9.14±0.07 and 8.97±0.18 for hNmU-R1 and hNmU-R2 respectively. Where applicable, cells were treated with 100ng ml^{-1} pertussis toxin (PTX) for 24hr prior to agonist challenge (filled symbols). [^{3}H]-InsP$_x$ accumulations are presented as the percentage increase relative to basal levels. Data are mean±s.e.m., n=3.

Figure 3. hNmU-R1- and hNmU-R2-mediated accumulation of Ins(1,4,5)P$_3$. a) Wild-type HEK293 cells (▲) or cells expressing either hNmU-R1 (□) or hNmU-R2 (o) were cultured on 24-well plates and challenged with 10nM hNmU-25 for the time shown before extraction and determination of Ins(1,4,5)P$_3$ using a radioreceptor assay. Data are mean±s.e.m, n=3. Cells expressing hNmU-R1 (b) or hNmU-R2 (c) were cultured on glass coverslips, transiently transfected with the eGFP-PH$_{PLC\delta1}$ construct and imaged by confocal microscopy. Cells were challenged with 10nM hNmU-25 at 15s. Changes in cytosolic fluorescence (as an index of Ins(1,4,5)P$_3$ levels) were

averaged from 6 cells chosen at random in the field of view but were representative of all cells. Images A, B and C were taken at the time points indicated on the graphs. Data are representative of at least 3 separate experiments.

Figure 4. hNmU-R1- and hNmU-R2-mediated changes in $[Ca^{2+}]_i$. hNmU-R1 (a) or hNmU-R2 (b) expressing cells were cultured on glass coverslips, loaded with fluo-3-AM and cytosolic fluorescence determined by confocal microscopy as an index of $[Ca^{2+}]_i$. Cells were challenged with 10nM hNmU-25 at 30s. Traces show the average change in cytosolic fluorescence of 6 cells in the field of view chosen at random. Image panels A, B and C were taken at the time points indicated on the traces. Data are representative of at least 4 separate experiments. c-f) $[Ca^{2+}]_i$ in cell populations was determined using fluo-4-loaded cells and a FLIPR. The time-course of 10nM hNmU-25-mediated changes in fluorescence intensity units (F.I.U) as an index of $[Ca^{2+}]_i$ is shown for cells expressing either hNmU-R1 (c) or hNmU-R2 (d). The concentration-response relationships for hNmU-25-mediated peak elevations of $[Ca^{2+}]_i$ in cells expressing either hNmU-R1 (e) or hNmU-R2 (f) gave pEC_{50} values of 9.41±0.09 and 9.37±0.06 respectively Data are mean±s.e.m., n=3.

Figure 5. hNmU-R-mediated inhibition of forskolin-stimulated cAMP accumulation. Cells expressing either hNmU-R1 or hNmU-R2 were cultured on poly-D-lysine-coated 24-well plates. hNmU-25 was added for 10min prior to addition of 10μM forskolin. Following a further 10min incubation, cAMP was extracted and measured by radioreceptor assay. Shown on the left of the panel are basal and forskolin-stimulated levels of cAMP in cells expressing either hNmU-R1 or hNmU-R2. On the right of the panel are curves showing the concentration-dependence of the hNmU-25-mediated inhibition of forskolin-stimulated cAMP accumulation. The pEC_{50} values for inhibition were 10.10±0.16 for hNmU-R1 (□) and 10.06±0.17 for hNmU-R2 (o). Following pertussis toxin-treatment of cells (PTX; 20hr, 100ng ml^{-1}), 10nM hNmU-25 failed to inhibit forskolin-stimulated cAMP accumulation in cells expressing either hNmU-R1 (■) or hNmU-R2 (●). All data are mean±s.e.m., n=3.

Figure 6. Activation of ERK by hNmU-R1 or hNmU-R2. Cells expressing either hNmU-R1 (a) or hNmU-R2 (b) were cultured on poly-D-lysine-coated 24-well plates

and stimulated with 10nM hNmU-25 for up to 60min. Levels of ERK were determined by Western blotting (a(i); hNmU-R1 and b(i); hNmU-R2) before being stripped and re-probed for phosphorylated ERK (pERK) (a(ii); hNmU-R1 and b(ii); hNmU-R2). Data are representative of 4 separate experiments. The density of pERK following stimulation of hNmU-R1 (□) or hNmU-R2 (○) was then related to the corresponding ERK density (c) using a Syngene Genegenius Bioimaging System. Data are mean±s.e.m, n=4.

Figure 7. $[Ca^{2+}]_i$ responses to repeated application of hNmU-25 in cells expressing either hNmU-R1 or hNmU-R2. Cells were cultured on glass coverslips, loaded with fluo-3 and cytosolic fluorescence measured as an index of $[Ca^{2+}]_i$ using confocal microscopy. Cells expressing either hNmU-R1 (a) or hNmU-R2 (b) were challenged with 10nM hNmU-25 at 30s. In panel c, cells expressing hNmU-R1 were challenged with 100μM carbachol at 30s. In each case, cells were perfused at 60s with agonist-free buffer for a further 120s. At 180s, either 10nM hNmU-25 (a and b) or 100μM carbachol (c) were re-applied. Changes in cytosolic fluorescence of all cells in the field of view were averaged and expressed relative to basal levels. Images A, B, C and D, were taken at the time points indicated. Data are representative of at least 4 experiments.

Figure 8. $[Ca^{2+}]_i$ responses to repeated application of hNmU-25 and UTP in smooth muscle cells isolated from rat fundus. Smooth muscle cells were dissociated from rat stomach fundus and cultured on glass coverslips for 5 days. Cells were loaded with fluo-3 and cytosolic fluorescence measured as an index of $[Ca^{2+}]_i$ using confocal microscopy. Cells were challenged with either 300μM UTP (a) or 10nM hNmU-25 (b) at 30s. In further experiments, naïve cells were challenged with either 100μM UTP (c) or 10nM hNmU-25 (d) at 30s and at 60s cells were perfused with agonist-free buffer. At 180s, 300μM UTP (c) or 10nM hNmU-25 (d) were re-applied. Changes in the cytosolic fluorescence of 3-6 cells within the field of view were plotted individually. In panel a, fluorescent images A, B and C were taken at the points indicated on the graph. All data are representative of at least 3 experiments.

Figure 9. hNmU-25-mediated accumulation of [^{3}H]-InsP$_x$ is unaffected by washing to remove extracellular hNmU-25. Wild type HEK293 cells (b) or cells expressing hNmU-R1 (a) were cultured in 24-well plates and loaded with *myo*-[^{3}H]-inositol for 48h before challenge with 10nM hNmU-25 in the presence of a 10mM Li^+-block of inositol monophosphatase activity. Cells were challenged with 10nM hNmU-25 (a) or 100μM carbachol (b) and after 10min were either untreated (●) or the buffer removed and the cells washed (three times with 1ml buffer) before replacement of buffer either without (○) or with (▼) agonist. Data are mean±s.e.m, n=3.

Figure 10. Cross-talk between receptors resulting in enhanced $[Ca^{2+}]_i$ signaling. Cells were cultured on glass coverslips, loaded with fluo-3 and cytosolic fluorescence measured as an index of $[Ca^{2+}]_i$ using confocal microscopy. Wild type HEK293 cells were challenged with 100μM carbachol at 30s to activate endogenous $G\alpha_q$-coupled muscarinic-M_3 receptors, followed by 10μM noradrenaline at 150s to activate endogenous $G\alpha_s$-coupled β_2-adrenoceptors. Noradrenaline was applied either in the continued presence of carbachol (a) or following a 120s wash with buffer (b). HEK293 cells expressing hNmU-R1 were challenged with 10nM hNmU-25 at 30s followed by 10μM noradrenaline either in the continued presence of hNmU-25 (c) or following a 120s wash with buffer (d). Changes in cytosolic fluorescence of all cells in the field of view were averaged and expressed relative to basal levels. All experiments are representative of 3 experiments. The experiments in (c) and (d) were repeated using cells expressing hNmU-R2 and similar data were obtained (not shown).

Figure 11. Binding of fluorescently-tagged NmU-8 to cells expressing hNmU-R1. Cells expressing hNmU-R1 were cultured on glass coverslips and imaged using confocal microscopy. Phase image (a(i)) and fluorescence image (a(ii)) of cells following addition of 10nM NmU-8-Cy3B. Fluorescence image of cells following addition of 10nM NmU-8-Cy3B (b(i)) and the same cells following addition of 1μM hNmU-25 (b(ii)). NmU-8-Cy3B (10nM) was added to cells at 0s (c(i)) and the cells were then perfused with buffer (5ml min^{-1}) for 700s (c(ii)) at 12^{o}C. Phase image (d(i)) and fluorescence image (d(ii)) of cells that were exposed to 10nM NmU-8-Cy3B following addition of (and in the continued presence of) 1μM hNmU-25.

Fluorescence image of NmU-8-Cy3B at 37^{o}C, at either 180s (e(i)), 300s (e(ii) or 600s (e(iii)). All images are representative of at least 3 separate experiments. Identical experiments were performed using cells expressing hNmU-R2 with identical results (data not shown).

Molecular Pharmacology Fast Forward. Published on August 26, 2004 as DOI: 10.1124/mol.104.002337
This article has not been copyedited and formatted. The final version may differ from this version.

Agonist	hNmU-R1	hNmU-R2
Human NmU-25	9.14 ± 0.07	8.97 ± 0.18
Porcine NmU-8	8.81 ± 0.09	8.70 ± 0.05
Porcine NmU-8-Cy3B	8.88 ± 0.09	8.79 ± 0.06

Table 1. Comparative pEC_{50} values of porcine NmU-8-Cy3B, human NmU-25 and porcine NmU-8 for [^{3}H]-$InsP_x$ accumulation mediated by recombinantly expressed hNmU-R1 or hNmU-R2.

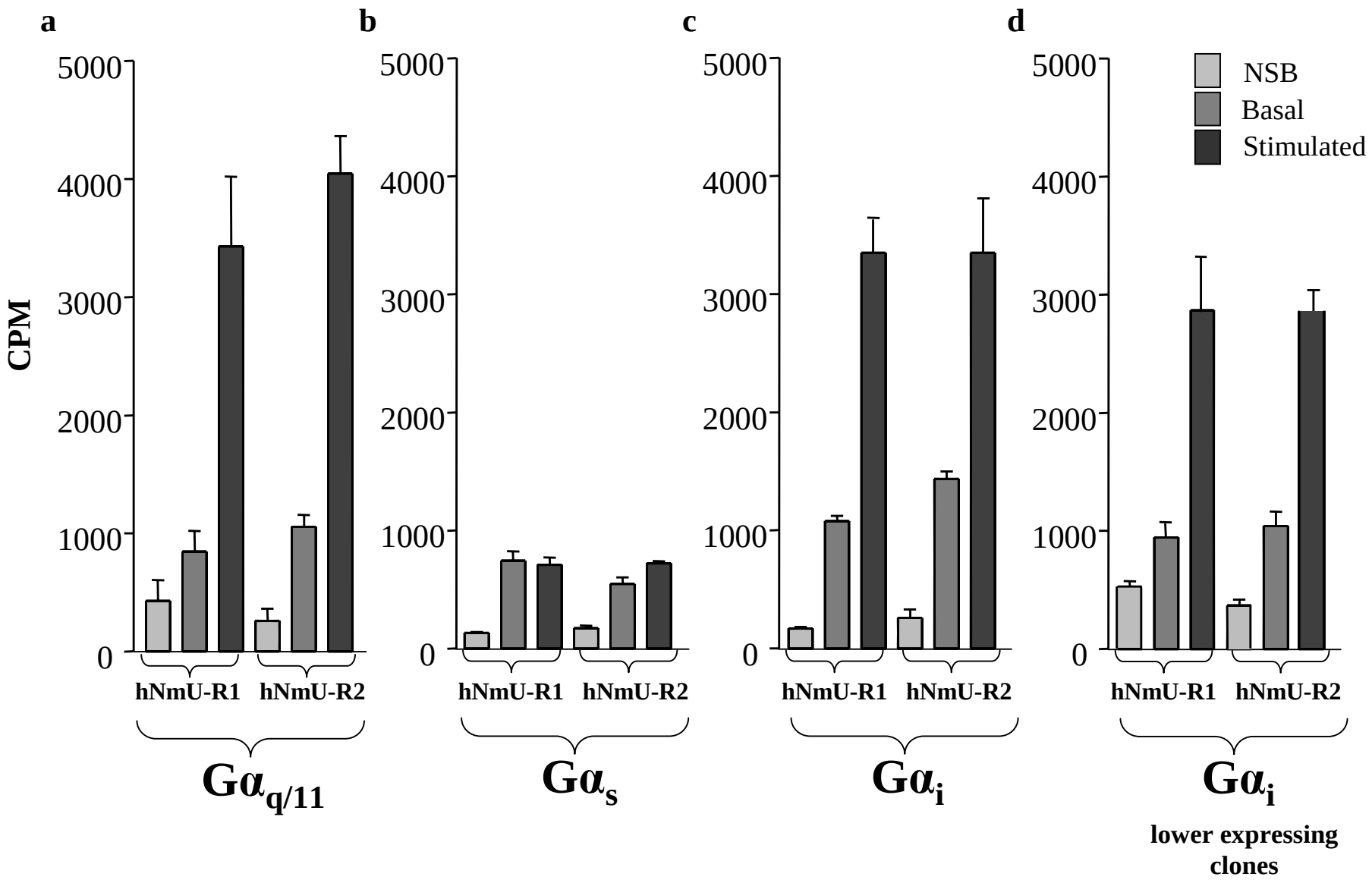

Fig. 1

Fig. 2

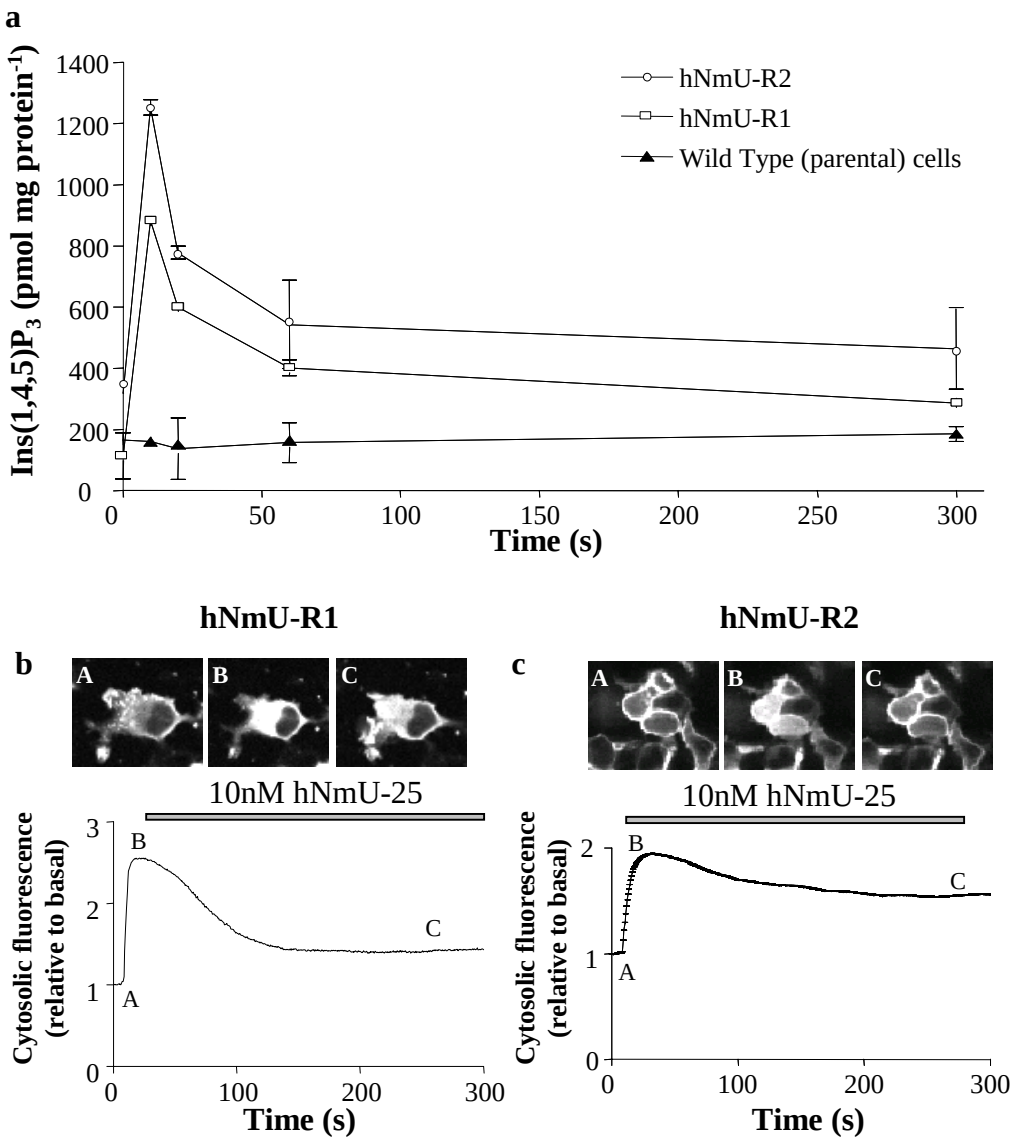

Fig. 3

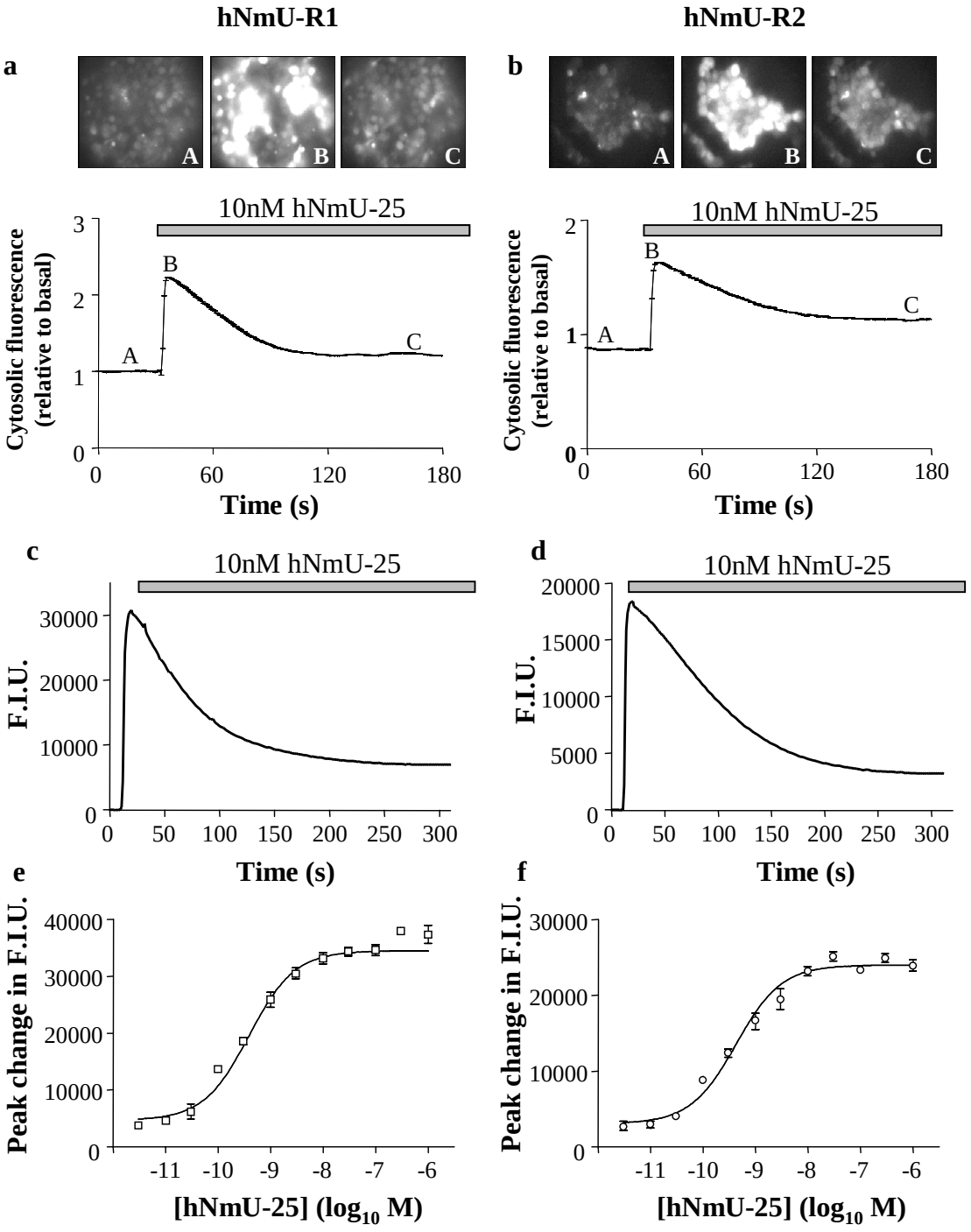

Fig. 4

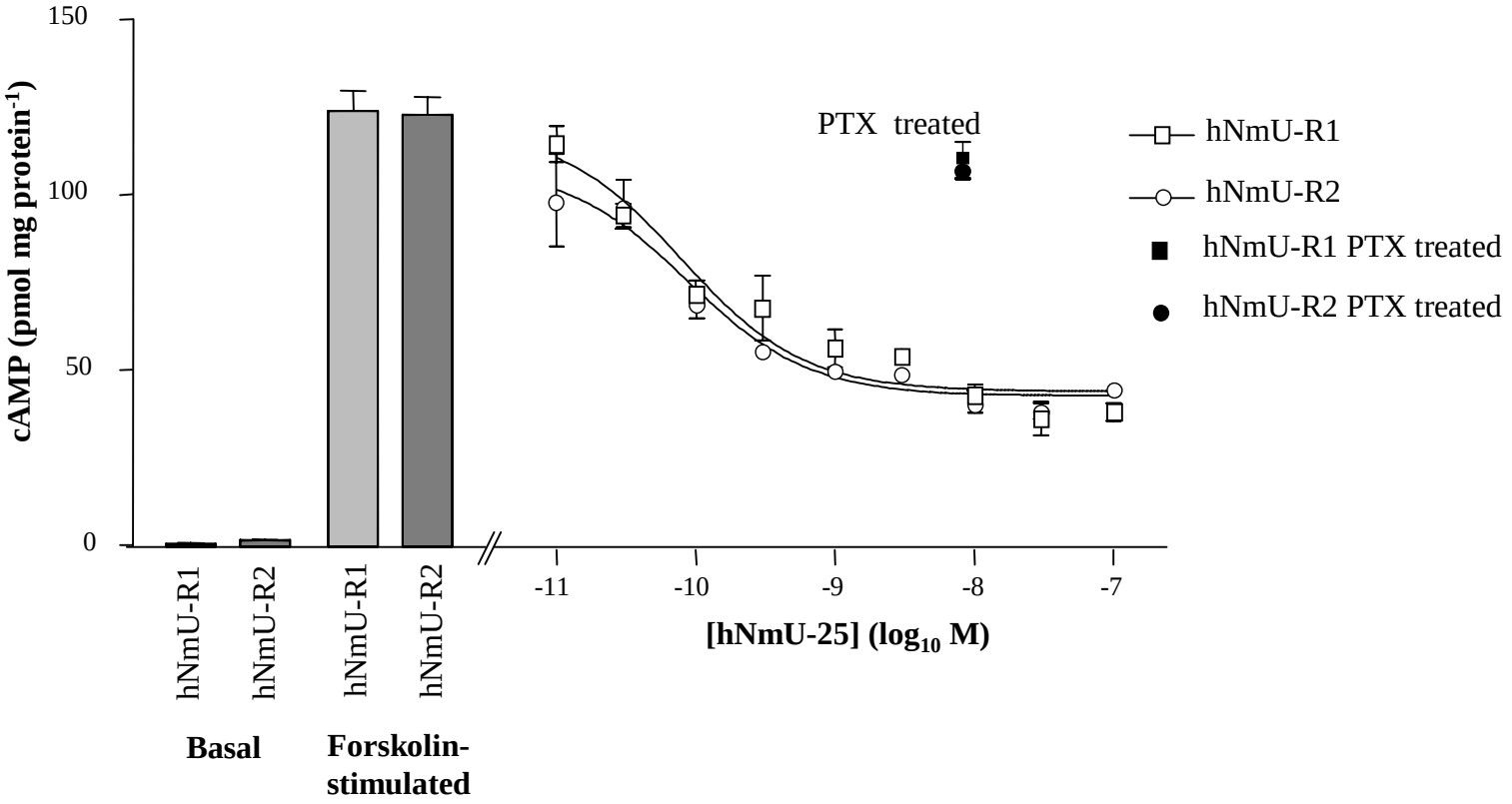

Fig. 5

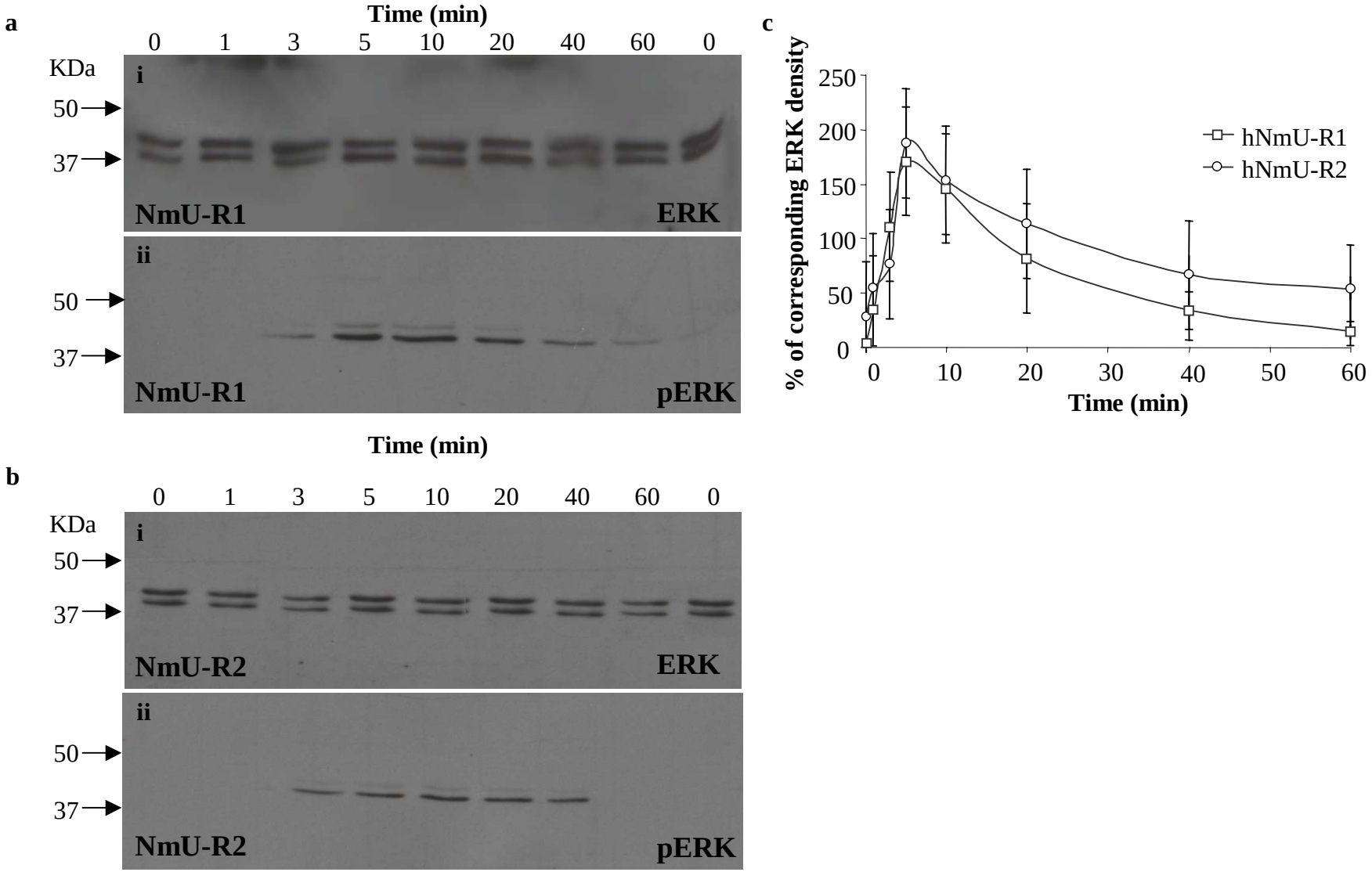

Fig. 6

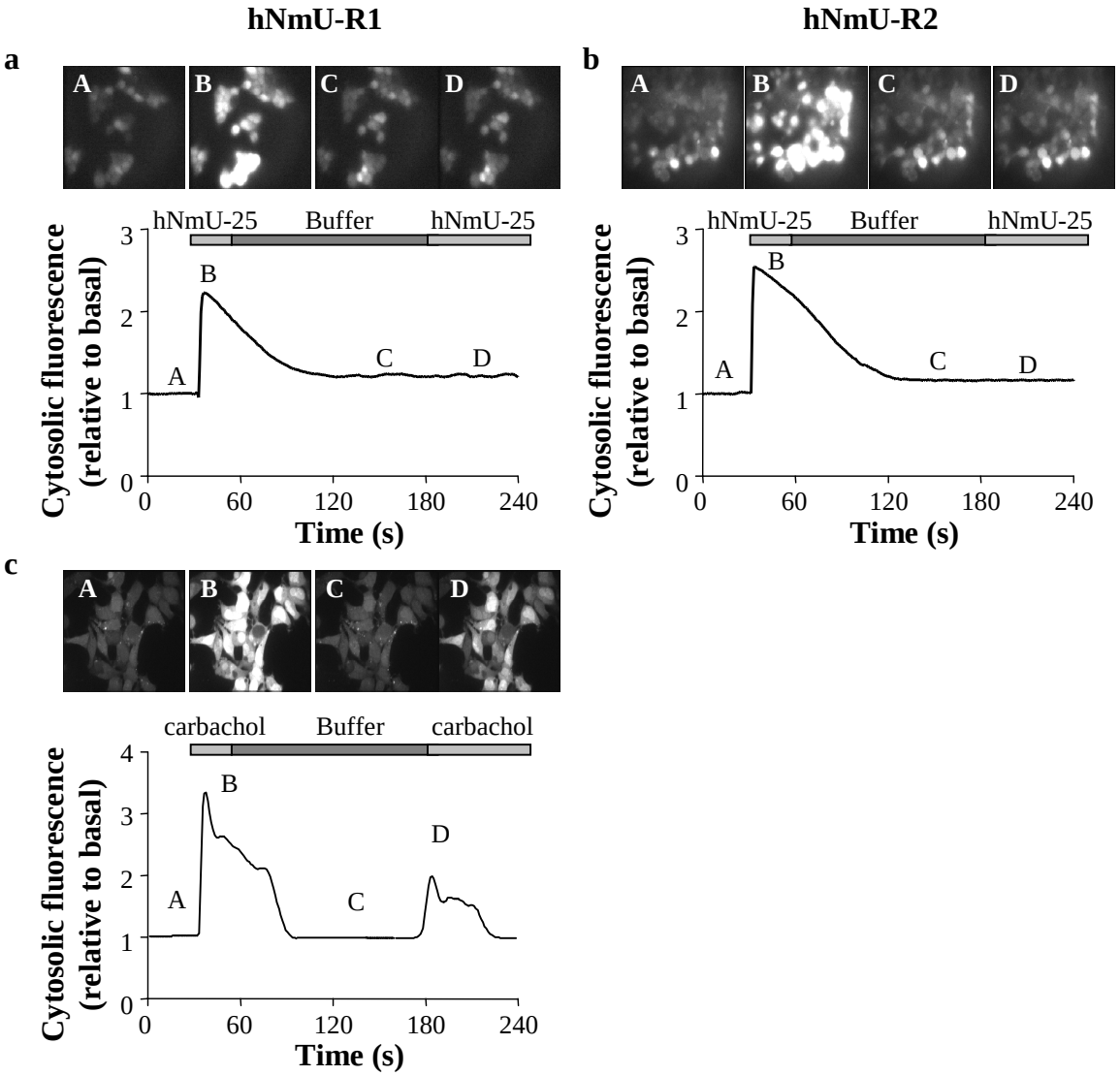

Fig. 7

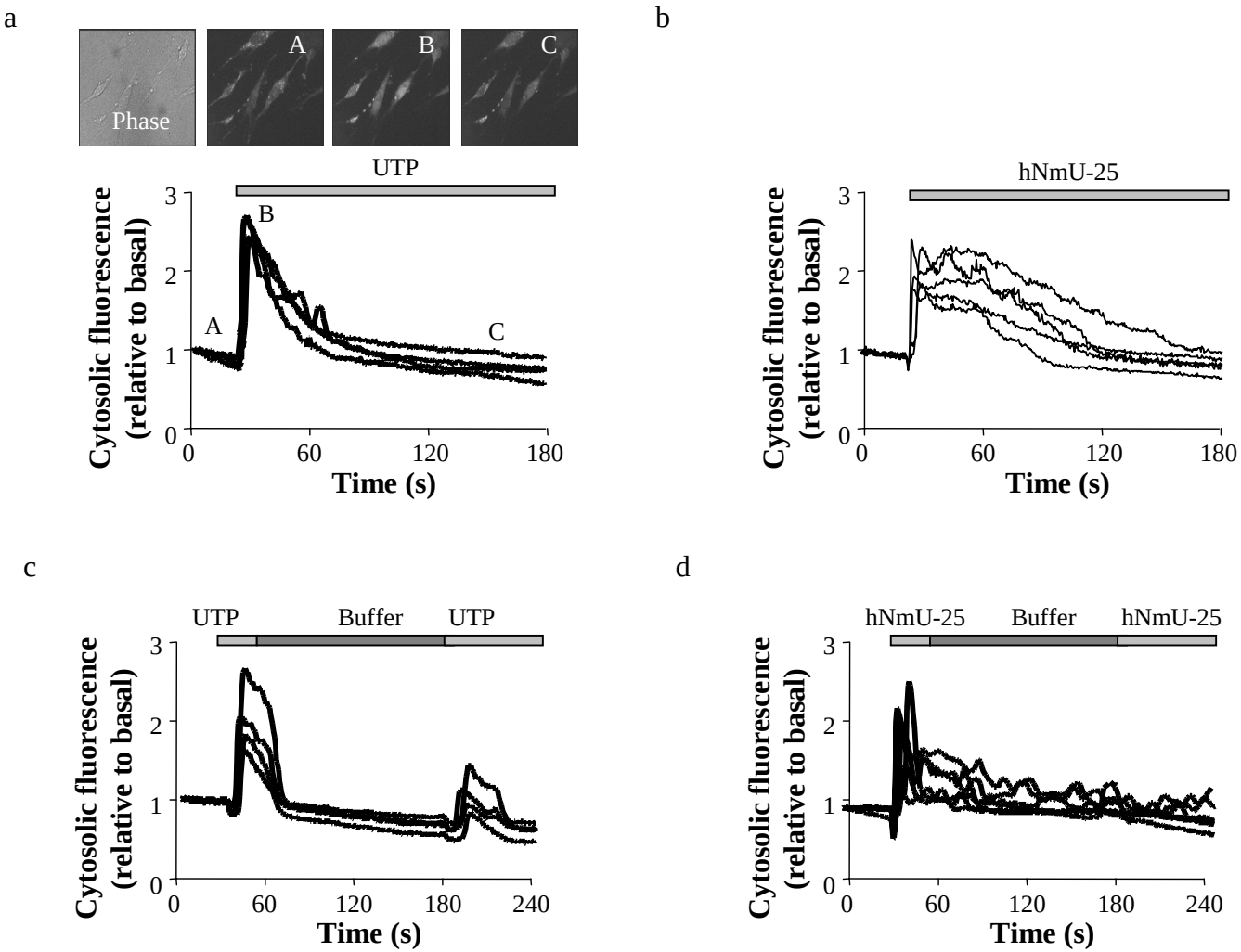

Fig. 8

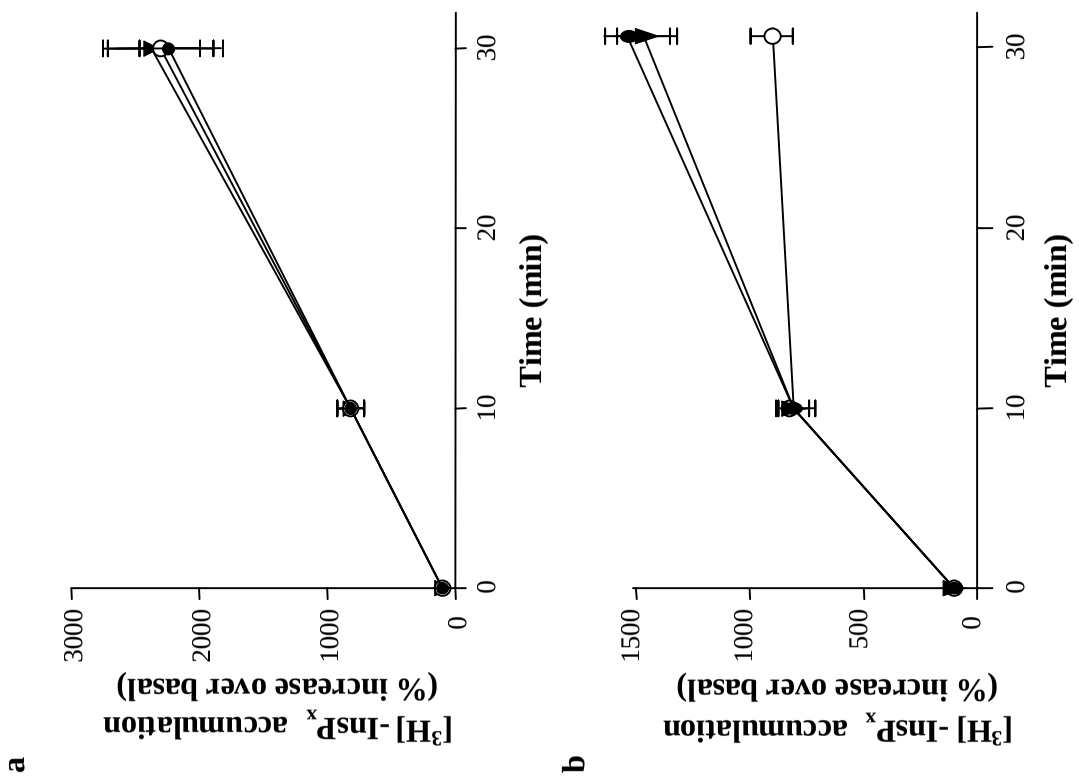

Fig. 6

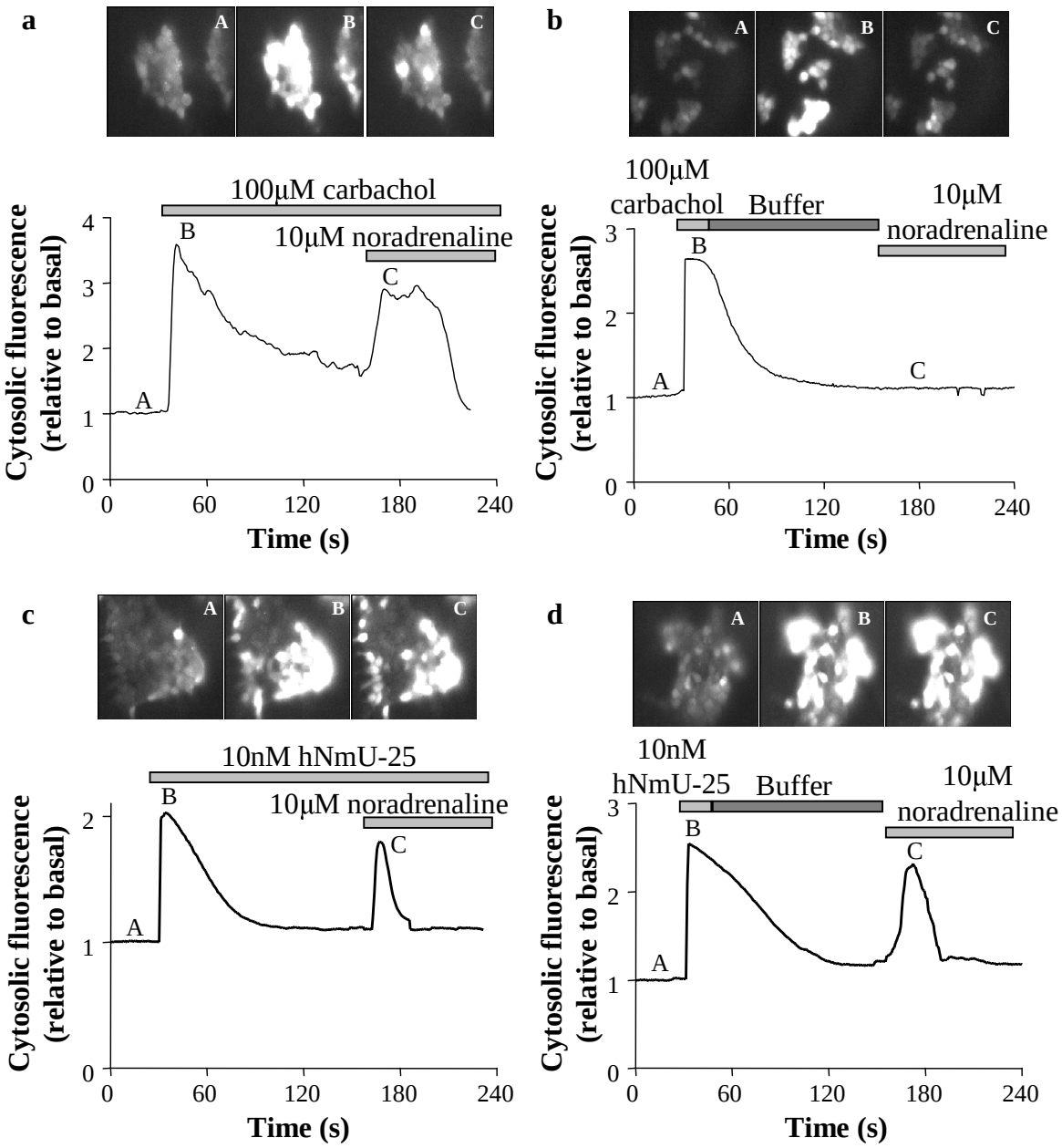

Fig. 10

Fig. 11